REMOVAL OF HEAVY METALS FROM WASTEWATER USING MULTIWALLED CARBON NANOTUBES

by

Malaz Suliman

A Thesis presented to the Faculty of the
American University of Sharjah
College of Engineering
In Partial Fulfillment
of the Requirements
for the Degree of

Master of Science in
Chemical Engineering

Sharjah, United Arab Emirates

April 2017

Approval Signatures

We, the undersigned, approve the Master's Thesis of Malaz Suliman.

Thesis Title: Removal of Heavy Metals from Wastewater Using Multiwalled Carbon Nanotubes.

Signature **Date of Signature**

(dd/mm/yyyy)

_____ _____

Dr. Taleb Ibrahim
Professor, Department of Chemical Engineering
Thesis Advisor

_____ _____

Dr. Zarook Shareefdeen
Professor, Department of Chemical Engineering
Thesis Committee Member

_____ _____

Dr. Kazi Fattah
Assistant Professor, Department of Civil Engineering
Thesis Committee Member

_____ _____

Dr. Mustafa Khamis
Professor, Department of Biology, Chemistry and Environmental Sciences
Thesis Committee Member

_____ _____

Dr. Naif Darwish
Head, Department of Chemical Engineering

_____ _____

Dr. Mohamed El-Tarhuni
Associate Dean for Graduate Affairs and Research, College of Engineering

_____ _____

Dr. Richard Schoephoerster
Dean, College of Engineering

_____ _____

Dr. Khaled Assaleh
Interim Vice Provost for Research and Graduate Studies

Acknowledgements

I would like to thank my advisor Dr. Taleb Ibrahim for his help and guidance throughout this work. I am also grateful to the Chemical Engineering Department at the American University of Sharjah for the Graduate Teaching Assistantship.

I am thankful to Dr. Mustafa Khamis for his help and suggestions. I am also thankful to Mr. Ziad Sara and Mr. Nedal Abu-Farha who provided useful training on using different laboratory apparatuses and instruments.

Finally, I am deeply grateful to my family for their unlimited support throughout my life.

Abstract

Recently, carbon nanotubes have been employed as new adsorbent for the removal of many pollutants. In this study, raw multiwalled carbon nanotubes (MWCNTs) were firstly tested for the removal of lead from aqueous solutions. Then, sodium lauryl sulfate modified multiwalled carbon nanotubes (SLS-MWCNTs) were produced, characterized and used for lead removal. Surface characterization using energy dispersive X-ray spectroscopy (EDS), thermogravimetric analyzer (TGA) and Fourier transform infrared spectroscopy (FTIR) showed that surface modification has been achieved successfully. Adsorption results revealed that the surface modification has increased the adsorption capacity from 3.84 mg/g for raw-MWCNTs to 141 mg/g for SLS-MWCNTs. On the other hand, the optimum values of some important parameters were determined. Optimum values of adsorbent dosage, contact time, pH and temperature using raw-MWCNTs were found to be 15.0 g/L, 50 min, 6.5 and 25℃, respectively and for the SLS-MWCNTs the optimum parameters were found to be 3.00 g/L, 30 min, 5.3 and 25℃, respectively. Fitting equilibrium data on different isotherm models showed that adsorption on raw-MWCNTs follows Langmuir model with q_m = 3.84 mg/g and K_L = 0.29 L/mg, while adsorption on SLS-MWCNTs is best described by Freundlich model with n = 2.50 and K_F = 15.40 ($mg^{0.6}$. $L^{0.4}$)/g. Furthermore, kinetics study results revealed that both raw and SLS-MWCNTs follow the pseudo second order model with rate constants 0.11 g/mg.min and 0.06 g/mg.min, respectively. Thermodynamics study showed that mode of adsorption is physisorption on both raw and SLS-MWCNTs with ΔG values -0.45 and -9.21 kJ/mol at 25℃, respectively. In order to get higher density particles with more granular structure to enhance column operation, magnetite pellets of SLS-MWCNTs were prepared and used in packed bed column. Column data were found to fit well by the modified dose response model with parameters values q_{mdr} = 28.4 mg/g and a' = 3.47 mg^{-1}.

Search Terms: ***Multiwalled carbon nanotubes; sodium lauryl sulfate; lead; adsorption; Isotherms; Kinetics.***

Table of Contents

List of Figures

List of Tables

Nomenclature

a'	MDR model constant (mg^{-1})
A_T	Temkin isotherm equilibrium binding constant (L/g)
b_T	Temkin isotherm constant (mol/J)
C_a	Concentration of adsorbate on adsorbent at equilibrium (mg/L)
C_e	Equilibrium concentration of adsorbate (mg/L)
C_o	Initial concentration (mg/L)
C_t	Concentration at time t (mg/L)
k_{AB}	Adam-Bohart kinetic constant (L/mg.min)
k_{id}	Intra-particle diffusion rate constant (mg/g.h)
k_1	Lagergren rate constant of first order adsorption (min^{-1})
k_{Th}	Thomas kinetic coefficient (ml/min.mg)
k_{YN}	Yoon-Nelson rate constant (min^{-1})
k_2	Rate constant of second order adsorption (g/ mg.min)
K_c	The apparent equilibrium constant
K_{DR}	Dubinin–Radushkevich isotherm constant (mol^2/ kJ^2)
K_F	Freundlich indicative of relative adsorption capacity (g/mg)
K_{fd}	Liquid film diffusion constant (min^{-1})
K_l	Langmuir isotherm constant (L/mg)
m	Mass of adsorbent (g)
M	Weight of adsorbent per solution volume (g/ L)
n	Freundlich indicative of the intensity of adsorption
N_o	Saturation concentration from Adam-Bohart model (mg/L)
q_e	Adsorption capacity at equilibrium (mg/g)
q_m	Maximum adsorption capacity (mg/g)
q_s	The theoretical isotherm saturation capacity (mg/g)
q_t	Adsorption capacity at time t (mg/g)
Q	Fluid volumetric flow rate (ml/min)
R	The universal gas constant (8.314J/mol/K)
T	Temperature (°K)
t	Contact time (min)

U_o	Fluid velocity in the bed (cm/min)
V	Volume of the solution (mL)
z	Height of bed (cm)
α	Elovich initial adsorption rate (mg/g.min)
β	Elovich desorption constant (g/mg)
τ	Time required for 50% column breakthrough (min)
ΔG	Gibbs free energy change (kJ/mol)
ΔH	Enthalpy change (kJ/mol)
ΔS	Entropy change (kJ/mol.°K)

Chapter 1. Introduction

1.1. Background and Research Objectives

Mostly all industrial processes produce waste materials. They can be in the form of gaseous emissions, waste water or even solid waste. Examples for such waste materials are: solvents, organic compounds, petroleum products and heavy metals [1]. These waste materials are considered as contaminants for the environment. Nowadays, environmental pollution is one of the serious problems facing the world and the pollution levels have increased dramatically in the last years. It reached high levels which can affect living creatures [2]. Chemical industries which produce waste water contaminated with heavy metals such as arsenic (As), lead (Pb), zinc (Zn), nickel (Ni), copper (Cu), cadmium(Cd) and chromium (Cr) are considered amongst the most hazardous industries due to the highly toxicity and non-degradable nature of these metals [3, 4]. Therefore, heavy metal-contaminated waste water is faced with more stringent regulations and these toxic heavy metals should be removed or reduced to an acceptable level before discharge to the receiving water bodies [5, 6].
Many techniques are used in the treatment of wastewater contaminated with heavy metals. However, adsorption is the most widely used process because it is effective both technically and economically [6]. The need for more efficient adsorbents has necessitated research interest towards alternatives other than the conventional activated carbon [2]. Recently, carbon nanotubes (CNTs) have been studied as new adsorbents for the removal of heavy metals from water and the results of these studies showed that CNTs are effective adsorbents for selected heavy metals [7].

This work is mainly aimed to study the efficiency of using modified multiwalled carbon nanotubes (MWCNTs) as adsorbents in the removal of lead from waste water. The adsorption characteristics of pure MWCNTs will firstly be studied. Then a surface modification will be applied to the pristine MWCNTs, and a comparison will be conducted between results of both adsorbents. Furthermore, the optimum conditions required for the removal process including adsorbent dosage, contact time, solution pH and temperature will be determined.

1.2. Literature Review

1.2.1. Heavy metals: sources, effects and environmental regulations. Heavy metals or trace metals are the metallic elements of the periodic table. They have density exceed 6 g per cubic centimeter [8, 9]. Heavy metals have a non-biodegradable nature, in other words they tend to accumulate in living creatures [6]. Very small amounts of some of these heavy metals (e.g zinc, iron, copper) are required for the metabolism of human body. However, they become extremely toxic at higher concentrations [1, 2]. Humans can be exposed to heavy metals through inhalation of fume or dust, ingestion of food or drink and skin or eye contact [2, 5].

There are two main sources for heavy metals: (1) Natural sources: Heavy metals can be naturally found in the crust of the earth. Furthermore, soil erosion and volcanic activities are also considered as natural sources for heavy metals [2,10]; (2) Anthropogenic sources: industries such as glass, pesticides, fertilizers, paper, electronics, batteries, paints and mining operations are amongst main sources which discharge heavy metal-contaminated water to the environment [6,11].

The release of industrial waste water containing high concentrations of heavy metals to the environment without treatment has serious negative impacts on animals, plants, soil, aquatic life and humans. Heavy metals may affect the growth and development of animals and may also cause damage for their organs and nervous system. High concentrations of heavy metals in soil may reduce its quality hence inhibit plants growth which leads to reduction in food production [5]. With regard to plants, serious effects of heavy metals are observed. These include the inhibition of photosynthesis which results in reduction of plant growth and chlorophyll production and seed germination [12]. Negative impacts of heavy metals on aquatic life are severe due to their high solubility in aquatic systems. These impacts include habitat destruction, increased water flow and the eventual death of aquatic creatures [5]. Heavy metals can enter human body through food chain and accumulate in the tissues causing serious damage to cells and organs which may lead to death in rare cases [2, 8]. Lead is a non-biodegradable toxic heavy metal. Mainly, it enters human body through contaminated drinking water and then spread in the whole body through blood. Mining operations, paints and pesticides industries are main sources of lead [7].

One of the serious effects of lead on human body is its ability to replace calcium in bones and forming sites in the case of long term replacements [13]. Lead effect on children may last forever. It negatively affects child growth and learning ability. Furthermore, it is linked to anti-social and future crime behavior. It also causes problems in hemoglobin production, cellular process, central nervous system, kidneys, liver and brain functions. Symptoms of lead toxicity include: weakness of muscles, headache, dizziness and irritability [8, 14].

To protect human health, international organizations such as Environmental Protection Agency (EPA), World Health Organization (WHO) and the European Union Commission set limitations on the level of heavy metals in drinking water [13]. There is no expected risk to health below the maximum contaminant level goal (MCLG). Maximum contaminant level (MCL) is the maximum allowed level of heavy metals in drinking water. While MCLGs are non-enforceable limitations, MCL are strictly applied and enforced [11]. Table 1.1 summarizes the sources, MCL, MCLGs and health effect of selected heavy metals on human. In spite of all these limitations and guidelines, contamination of drinking water with heavy metals is still reported in some countries. In China, Bangladesh, Vietnam, Taiwan, Thailand, Nepal and India high concentrations of Arsenic were reported. In Africa and specifically in Ghana, contamination by arsenic, mercury and lead in drinking water were also reported [16].

1.2.2. Techniques used for the removal of heavy metals from water. To protect humans, living organisms and the environment from the serious negative effects of toxic heavy metals including lead, different technologies have been developed and used for the treatment of heavy metal-contaminated waste water. Examples for these technologies are: chemical precipitation, adsorption, coagulation and flocculation, flotation, ion exchange, membrane filtration, electrochemical treatment and bioremediation. Each technology has its advantages and disadvantages and the selection of specific process or technology depends mainly on the pH, the initial concentration of lead in the waste water as well as economic considerations such as capital and operational costs [3, 7]. More details about these techniques are discussed in following subsections.

Table 1.1: Main sources, health effects, MCL and MCLGs of selected heavy metals.

Heavy metal	Main sources	Health effects	EPA regulations		WHO guidelines (mg/L)	References
			MCL (mg/L)	MCLG (mg/L)		
As	1. natural deposits erosion 2. glass industry 3. electronics production waste	1. skin damage 2. circulatory systems problems 3. cancer	0.01	0	0.01	[11,17]
Cr	1. metal finishing 2. textile industry 3. chromate preparation 4. leather tanning	1. skin irritation 2. lung problems	0.1	0.1	0.05	[11,17,18,19]
Cd	1. paints industry 2. batteries industry 3. metal refineries discharge 4. galvanized pipes corrosion	1.bone defects 2.lung disease 3.increased blood pressure	0.005	0.005	0.003	[11,17,20]
Hg	1.natural deposits erosion 2.refineries discharge 3.landfills runoff	1. damage to nervous system 2.chest pain 3.damage to kidneys	0.002	0.002	0.006	[11,17,21]
Zn	1. sediment entrainment 2. ground water intrusion 3. agricultural activities	1.vomiting 2. nausea 3. anemia 4. stomach cramps 5. fever	-	-	-	[11,15,22]
Ni	1. mining 2. batteries manufacturing 3. metal finishing 4. galvanization	1. lung cancer 2. kidney diseases 3. dry cough 4. nausea	-	-	0.07	[11,17,23,24]
Cu	1. natural deposits erosion 2. plumping systems corrosion	1. kidney damage 2. liver cirrhosis 3.cramps 4. anemia 5. convulsions	1.3	1.3	2	[5,11,17, 25]
Pb	1. pesticides industries 2. paints industries 3. mining operations 4. natural deposits erosion	1. high blood pressure 2. kidneys problems 3. nervous system damage 4. problems in learning abilities for children	0.015	0	0.01	[7, 8, 11,17]

1.2.2.1. *Chemical precipitation*. Chemical precipitation is a conventional widely used process for the removal of heavy metals from aqueous solutions. It can also be used in combination with other technologies. It is usually used for the treatment of water containing high concentrations of heavy metals. However, it is not efficient when the level of heavy metals is low. Generally, chemical precipitation processes include using of precipitant chemical agents in order to react with the heavy metal ions forming an insoluble precipitates which can latterly be separated from the water using filtration or sedimentation. Lime is the most used available and cheap reagent. Hydroxide precipitation and sulfide precipitation are the most employed techniques of chemical precipitation. Merits of this method include simplicity and low capital cost. Regardless, this process needs large amounts of chemicals in order to reduce the level of heavy metals. Moreover, it discharges a huge amount of sludge which needs to be treated and has its long term negative impacts on the environment [3, 6, 7, 26]. Hydroxide precipitation is characterized by its low cost, simplicity and easiness of pH control. One of the major drawbacks of hydroxide precipitation is production of low density sludge which causes problems in dewatering and discharge. On the other hand, sulfide precipitation has the ability to remove heavy metals in a wider range of pH compared to hydroxide precipitation which could be attributed to its lower solubility compared to hydroxide precipitates. Moreover, sludge produced using sulfide precipitation has better dewatering characteristics than hydroxide precipitation [6].

1.2.2.2. *Ion exchange*. Ion exchange is another technology used for the removal of heavy metals. This technology includes using of natural or synthetic resins in order to exchange their cations with the heavy metals in water. Zeolites and silicate minerals are examples of natural low cost resins which have been widely used in the removal of heavy metals from waste water. Advantages of ion exchange include high removal efficiency. Nevertheless, resins used in this technology need to be regenerated when they are fouled using chemical reagents and this may cause another pollution issue. Moreover, ion exchange is expensive and cannot be used for the treatment of large amounts of waste water with low concentrations of heavy metal. Disadvantages of ion exchange also include non-selectivity and high sensitivity to the pH of the aqueous solution [3, 6, 27].

1.2.2.3. *Coagulation and flocculation*. Coagulation and flocculation are used in the removal of heavy metals from waste water. They are usually followed by sedimentation or filtration step. Alum ($KAl(SO_4)_2$. $12H_2O$), ferric chloride and ferrous sulfate are examples of coagulants used in the treatment of waste water. Disadvantages of coagulation and flocculation include high chemical consumption and production of high volume sludge. However, this produced sludge has good dewatering characteristics. In flocculation, flocculants are used in order to gather particles and form larger clumps which can be removed latterly using filtration or straining. Although there are many flocculants used in waste water treatment such as poly aluminium chloride (PAC), poly ferric sulfate (PFS) and poly acrylamide (PAM), they are ineffective in the removal of heavy metal from waste water. In general, coagulation and flocculation are not efficient in complete removal of heavy metals from waste water, thus, they must be followed by other techniques [6, 7, 28].

1.2.2.4. *Membrane filtration*. Membrane filtration is used for the removal of suspended solids and organic compounds as well as inorganic pollutants such as heavy metals. Although it has the advantages of high efficiency and space saving, it is not a widely used for the removal of heavy metals due to its high cost, complexity, low permeate flux and membrane fouling. Generally, membrane filtration technique utilizes a semi permeable membrane to allow the passage of aqueous solution and prevent pollutants. There are different types of membrane processes depending on the membrane size such as ultrafiltration, nanofiltration, reverse osmosis and electrodialysis. In ultrafiltration, a membrane of pore size 5-20 nm is used. The pores allow the passage of water while preventing dissolved contaminants which have size larger than the pore size [3, 29]. Nanofiltration has properties in between ultrafiltration and reverse osmosis. Low operating pressure, high flux and relatively low capital and operating costs are amongst main advantages of nanofiltration [30]. Electrodialysis is a membrane process used for the treatment of heavy-metals contaminated water. In this technique a charged membrane is used and an electric field is utilized as a driving force to separate ions. Two main types of membranes are usually used in this technology: anion-exchange membrane and cation-exchange membrane. While solution containing ions is passing through the membrane, anions move toward anode and cations toward cathode. Electrodialysis process is

characterized by its high separation selectivity. However, it has high operational cost due to high energy consumption [3, 6]. Reverse osmosis technique also consumes high power in pumping and membranes regeneration. Like other membrane technologies, a semi-permeable membrane is used in reverse osmosis to allow the passage of solution and prevent pollutants [6].

1.2.2.5. *Floatation*. Flotation is used for separation of heavy metals using bubble attachment [6]. In foam flotation a surfactant is used to convert a non-surface active material to surface active one. The new formed material can be removed by bubbling a gas through the bulk solution forming foam. Flotation is mainly used to treat waste water with very low concentrations of heavy metals (parts per billion or parts per million). It has the advantages of limited required space, flexibility, simplicity and production of low volume sludge [31]. The major drawback of floatation is high capital, operational and maintenance cost [7]. Major floatation processes used for the removal of heavy metals from waste water include: ion flotation, dissolved air flotation (DAF) and precipitation flotation [6].

1.2.2.6. *Electrochemical treatment*. Electrolytic metal recovery is another technique for heavy metals removal. It has been originally used in mining industry for metal electrorefining. Basically, in electrochemical methods a direct current is applied to the aqueous solution which contains heavy metal ions. Positively charged ions will move toward cathode leaving behind a metal residue which can be recovered through stripping [31]. Electrocoagulation, electroflotation and electrodeposition are amongst main electrochemical processes. Electrochemical treatment technologies are well controlled processes which produce low sludge, require few chemicals and yield effluent with acceptable level of heavy metals. However, electrochemical methods are not commonly employed due to their high capital cost and high electricity consumption [6].

1.2.2.7 *Bioremediation*. Bioremediation or microbial remediation is a relatively new process employed in the last years. It includes using of microorganisms such as bacteria, protozoan, fungi and yeast for the removal of heavy metals. The technique is based on reducing the heavy metal level through the biological activity of the used microorganism. Plants can also be used to reduce the

bioavailability of heavy metals in soil or water using a process called phytoremediation [5].

In this study, adsorption technique is used for lead removal due to its technical and economical merits over other methods. It is a widely used technology in the removal of heavy metals from water. It has a relatively low cost compared to other available techniques. Moreover, it is applicable for a wide pH range and it produces high quality effluent with an acceptable level of heavy metals even from low concentrated waste water. Adsorption technology has flexible design with easy operating conditions and minimum requirement for a control system. Furthermore, adsorption process is reversible and the used adsorbents can be regenerated and reused [2, 6, 7].

In the following sections adsorption theory, equilibrium, kinetics and thermodynamics will be discussed.

1.2.3. Adsorption. In all separation processes there is a difference in a specific property between components which represents the driving force for separation; adsorption occurs when there is a particular component which is readily to be adsorbed on a solid surface more than other components. In adsorption, an adsorbed phase is formed when molecules diffuse from a liquid or gas phase to a solid surface. This solid on which adsorption occurs is called adsorbent, while adsorbate is the component to be adsorbed. Adsorption is generally used to recover a specific component or to remove an undesirable one from an industrial effluent. Examples for adsorption applications in industry include: separation of paraffins from aromatics, separation of fructose from glucose using zeolites and removal of organic compounds from aqueous solutions. Adsorption is usually taken place in a bed packed with solid adsorbent. The fluid is passed through this bed and the component needs to be separated is adsorbed on the adsorbent surface. When the bed is saturated, it is taken for regeneration. After desorption process, the adsorbate is recovered and the adsorbent is ready to be used again. The limited capacity of adsorbents and their need to be regenerated between specific intervals have limited the application of adsorption in early industry. However, nowadays a variety of adsorbents have been developed for a wide range of separation applications [3, 32, 33].

Essentially, adsorption process is carried out in three major steps [34]:

(1) Film diffusion: diffusion of the adsorbate molecules from the bulk fluid to the adsorbent external surface.

(2) Particle diffusion: diffusion of the adsorbate molecules inside the pores of the adsorbent particle.

(3) Adsorption: adsorption of the adsorbate molecules on the adsorbent internal surface.

There are two types of adsorption, physical adsorption or Van der Waals adsorption and chemisorption. Physisorption is an exothermic process results in decrease of free energy. It takes place at temperatures lower or close to the critical temperature of the adsorbate. It usually occurs between adsorbate molecules and adsorbent internal pore surface as a result of Van der Waals forces. These forces are not strong enough and the process can easily be reversed. On the other hand, chemisorption is effective at temperatures much higher than the critical temperature. Moreover, there are other forces of a chemical nature binding the adsorbed molecules to the solid surface. Chemisorption process is not easily reversed; therefore, regeneration is much difficult compared to the case of physical adsorption. In some cases, both types of adsorption can occur at the same time [32, 33, 35].

1.2.3.1. ***Adsorption equilibrium*****.** Adsorption equilibrium is achieved when the adsorption rate of the adsorbate molecules on the adsorbent surface is equal to their desorption rate. The adsorbent capacity for a specific adsorbate depends on three factors: (1) temperature; (2) the concentration of the adsorbate in the fluid phase; and (3) the dosage of the solid. If one of these factors is kept constant, the remaining factors can be plotted to represent the equilibrium. It is common to keep the temperature constant and plot the adsorption capacity vs the equilibrium concentration of the adsorbate in the fluid phase. Such plot is called, adsorption isotherm [32, 33]. Adsorption isotherms provide information about adsorption mechanism and the adsorbent affinity. They are also important for the design of adsorption systems. Langmuir, Freundlich, Temkin and Dubinin-Radushkevich are examples for two parameter isotherm models [36].

1.2.3.1.1. *Langmuir isotherm model.* Langmuir adsorption isotherm model was developed by Langmuir in 1916. It is described by equation (1) below [37].

$$q_e = \frac{q_m K_L C_e}{1 + K_L C_e} \quad (1)$$

where: q_e is the amount of adsorbate adsorbed per gram of adsorbent at equilibrium (mg/g); q_m is maximum adsorption capacity (mg/g); K_L is Langmuir isotherm constant (L/mg) and C_e the equilibrium concentration of adsorbate (mg/L) [38]. Derivation of Langmuir model is based on some assumptions which are [33]:

1. Number of active sites available for adsorption is fixed
2. The adsorption reaches equilibrium
3. Only a monolayer is formed
4. The adsorption is reversible. Linearization of equation (1) gives the following equation [37]:

$$\frac{C_e}{q_e} = \frac{C_e}{q_m} + \frac{1}{q_m K_L} \quad (2)$$

Plotting C_e / q_e against C_e gives straight line with slope $1/ q_m$ and intercept $1/ q_m K_L$ if the adsorption data are described by Langmuir model.

1.2.3.1.2. *Freundlich isotherm model.* Freundlich isotherm model is based on a study of adsorption of organic compounds on charcoal in aqueous solutions. It is represented by equation (3). In this model, non-equal distribution of adsorption heat sites is assumed [32, 39].

$$q_e = K_F \, C_e^{\,1/n} \quad (3)$$

where: K_F is Freundlich indicative of relative adsorption capacity of adsorbent and n is Freundlich indicative of the intensity of adsorption [39]. K_F and n are constants which can be determined experimentally. The unit of K_F depends on n. By taking the logarithms for equation (3), it becomes:

$$Log\ q_e = Log\ K_F + \frac{1}{n} Log\ C_e \quad (4)$$

If plotting Log q_e versus log C_e gives straight line with slope 1/n and intercept log

K_F that means the data can be represented by Freundlich model.

1.2.3.1.3. *Temkin isotherm model.* Temkin isotherm is based on the assumption that heat of adsorption decreases linearly with the increase in coverage of the solid surface. Temkin isotherm is written in the following form [38]:

$$q_e = \frac{RT}{b_T} Ln\, A_T\, C_e \quad (5)$$

Linearization of equation (4) makes it as follow:

$$q_e = \frac{RT}{b_T} Ln\, A_T + \frac{RT}{b_T} Ln\, C_e \quad (6)$$

where: A_T is Temkin isotherm equilibrium binding constant (L/g); b_T is Temkin isotherm constant; R is the universal gas constant (8.314J/mol/K); T is Temperature (°K), C_e is the equilibrium concentration of adsorbate (mg/L) and q_e is the amount of adsorbate adsorbed at equilibrium (mg/g) [38].

1.2.3.1.4. *Dubinin-Radushkevich isotherm model.* The Dubinin-Radushkevich isotherm model is another two-parameter model used to describe adsorption data. The nonlinear form of Dubinin-Radushkevich isotherm model is as follows [37]:

$$q_e = q_s\, exp\, [- K_{DR} \epsilon^2] \quad (7)$$

The linear form of Dubinin-Radushkevich isotherm model is as follows [38]:

$$Ln\, q_e = Ln\, q_s - K_{DR} \epsilon^2 \quad (8)$$

$$\epsilon = RT\, Ln\, [1 + \frac{1}{C_e}] \quad (9)$$

where: q_e is the amount of adsorbate in the adsorbent at equilibrium (mg/g); q_s is the theoretical isotherm saturation capacity (mg/g); K_{DR} is Dubinin–Radushkevich isotherm constant (mol²/ kJ²), R is the universal gas constant (8.314 J/mol.°K); T is the absolute temperature (°K) and C_e adsorbate equilibrium concentration (mg/L) [38].

1.2.3.2. Adsorption kinetics. While studying adsorption equilibrium is essential to predict the effectiveness of the adsorption process for a given system, studying adsorption kinetics is important in determining the rate at which adsorption process takes place. It is essential for determining the adsorbate residence time and

the system design. There are many models which have been developed in order to identify the adsorption kinetics of a specific system. Some of these models are presented below [40, 41]:

1.2.3.2.1. *Pseudo- first order model.* The linear form of the pseudo- first order equation as given by Langergren and Svenska (1898) is as follows:

$$Ln\,(q_e - q_t) = Ln\,q_e - k_l\,t \qquad (10)$$

where: q_e and q_t are amounts of adsorbate adsorbed per gram of adsorbent at equilibrium and time t respectively (mg/g); and k_l is the Lagergren rate constant of first order adsorption (min^{-1}) which can be obtained from plotting $Ln\,(q_e - q_t)$ vs t [34, 42].

1.2.3.2.2. *Pseudo- second order model.* The pseudo- second order kinetic model can be written in the following linear form:

$$\frac{t}{q_t} = \frac{1}{k_2 q_e^{\,2}} + \frac{t}{q_e} \qquad (11)$$

where: k_2 is the rate constant of second order adsorption (g/ mg.min) which can be obtained from the intercept of the linear plot of t/q_t vs t [34, 42].

1.2.3.2.3. *Elovich model.* The linear form of this model is as follows:

$$q_t = \frac{\mathrm{Ln}\,\alpha\beta}{\beta} + \frac{\mathrm{Ln}\,t}{\beta} \qquad (12)$$

where: α is the initial adsorption rate (mg/g.min) and β is the desorption constant (g/mg). If the adsorption fits Elovich's model, a plot of q_t vs Ln t will give a straight line with slope $1/\beta$ and intercept $(Ln\,\alpha\beta)/\beta$ [40].

1.2.3.3. *Adsorption mechanism.* As discussed in Section 1.2.3, adsorption process involves three major steps and in order to determine which step is the rate limiting; some models were developed. Since the adsorption step is considered to be very fast, either film diffusion or particle diffusion will be the slowest. If the external (film) diffusion is faster than the internal diffusion, this means particle (internal) diffusion is the controlling step and vice versa. However, if they are equal, then at a

specific rate the diffusion of adsorbate molecules to the interface is impossible [34, 43].

1.2.3.3.1. *Intra-particle diffusion model.* The intra-particle diffusion model is used to determine the adsorption controlling step. It is an empirical functional relationship based on theory developed by Weber and Morris (1962) and it can be expressed as follows [34]:

$$q_t = k_{id}\, t^{1/2} + C \tag{13}$$

where: q_t is the amount of adsorbate adsorbed at time t (mg/g); k_{id} is the intra-particle diffusion rate constant (mg/g h); and t is the contact time (h). k_{id} and C are the slope and the intercept of the linear plot of q_t vs $t^{1/2}$. If the plot of the experimental data of q_t vs $t^{1/2}$ for a given system is linear and passes through the origin, this means the intra-particle diffusion is the limiting step. However, if the plot does not pass through the origin, then there are other mechanisms contributing in the controlling step. Moreover, large value of the intercept indicates higher contribution of surface sorption in the limiting step [42].

1.2.3.3.2. *Liquid film diffusion model.* This model is given by the following equation [44]:

$$Ln\,[1-F] = -K_{fd}\, t \tag{14}$$

$$F = \frac{q_t}{q_e} \tag{15}$$

where: q_t and q_e are the amount of adsorbate adsorbed at time t and equilibrium respectively (mg/g); and K_{fd} is liquid film diffusion constant. If plotting –Ln (1-F) vs t resulted in straight line passing through the origin, then liquid film diffusion is the limiting step [44].

1.2.3.3.3. *Bangham model.* Bangham's model is expressed as follows:

$$Log\left[\frac{C_0}{C_0 - q_t\, M}\right] = Log\left[\frac{K_0\, M}{2.3\, V}\right] + a\, Log\, t \tag{16}$$

where: C_o is initial concentration (mM), V is volume of the solution (mL), M is weight of the adsorbent per solution volume (g/L), q_t is amount of adsorbate retained

at time (t) (mmol.g^{1}) and a & K_o are constants. If plotting log [C_o / (C_o - q_t M)] vs log t gives straight line, then the controlling step is the pore-diffusion step [45].

1.2.3.4. ***Adsorption thermodynamics.*** Calculation of some thermodynamics parameters is important to fully understand any adsorption process. These parameters include Gibbs free energy change (ΔG), enthalpy change (ΔH) and entropy change (ΔS). The adsorption free energy is calculated as follows [46, 47]:

$$\Delta G = \Delta H - T\,\Delta S \tag{17}$$

Equation (18) below is used to get the enthalpy and entropy. They can be found from the slope and intercept of the linear plot of Ln K_c versus 1/T plot.

$$Ln\,K_c = Ln\left(\frac{Ca}{Ce}\right) = \frac{\Delta S}{R} - \frac{\Delta H}{RT} \tag{18}$$

where: K_c is the apparent equilibrium constant, C_a is the concentration of adsorbate on adsorbent at equilibrium (mg/L), C_e is the concentration of adsorbate in solution at equilibrium (mg/L), R is the universal gas constant and T is the absolute temperature (°K) [46, 47]. The sign of the enthalpy indicates whether the process is endothermic or exothermic and the sign of the entropy gives information about the degree of freedom of the adsorbate [47]. On the other hand, negative value of Gibbs energy suggests that the adsorption process is spontaneous [46].

1.2.4. Adsorbents. Typically, adsorbents can be in the form of granules, extruded pellets, beads or formed spheres. They have porous structure with pore volumes represent up to 50% of the total particle volume. Adsorbents can be industrial by-products, biomass, agricultural waste, polymeric materials or materials of organic or biological origin. Examples for commercial adsorbents include: activated carbon, silica gel, activated alumina and zeolites. Commercial adsorbents have main characteristics which include [32, 33, 48]:

(1) Large surface area.

(2) Porous structure with pores size suitable to admit molecules to be adsorbed and reject others.

(3) Can easily be regenerated.

(4) Mechanically strong to withstand the harsh industrial conditions.

(5) Long age to withstand regeneration and reusing without losing its adsorptive capacity.

The most frequently used adsorbent in industrial waste water treatment is activated carbon. It can be made by thermal decomposition of carbonaceous materials such as coal, wood, bones, vegetables shells, coconut shells, etc at a temperature of 800 °K. After that, an activation process is required to generate pores. Activation includes oxidation at temperatures greater than 1000 °K in the presence of materials such as steam or carbon dioxide. Activated carbon can be directly produced from raw material when it is treated with chemicals such as phosphoric acid or zinc chloride. It has a surface area ranges between 300 – 1200 m^2/g and pores of about 2 nm in diameter. It can be used in granular form or powder to adsorb components from gases or aqueous solutions. When it is used in powder form, it is mixed with the solution to be treated and then filtered. Granular activated carbon has a low affinity to water and it can be regenerated [32, 33].

Commercial activated carbon is considered as a relatively expensive material, thus, there is an urgent need for other effective and low-cost adsorbents to be used in the removal of heavy metals from waste water. An adsorbent is considered to be low cost adsorbent when it is abundantly available in nature or it is a by-product or waste of an industry. In the last years, many natural and agro-based adsorbents have been studied by researchers. Biosorbents are agricultural waste or by-products utilized for the removal of heavy metals in a process called biosorption. Biosorbents such as hazelnut shell, rice husk, pecan shells and husk can be used for waste water treatment after conversion into activated carbon. Industrial by-products such as fly ash, hydrous titanium oxide, waste iron and iron slags have also been studied as new adsorbents and alternatives to commercial activated carbon [1, 2, 3, 6].

In this study, multiwalled carbon nanotubes (MWCNTs) is used as adsorbent. This material is chosen due to its excellent and exceptional properties. MWCNTs have large surface area, hollow and layered structure which makes them perfect for adsorption. Also, their surface has the ability to be further modified in order to improve their dispersibility, increase the surface area and consequently enhance adsorption [6, 7, 49]. Compared to single walled carbon nanotubes (SWCNTs), MWCNTs are much cheaper and more pure. Furthermore, their multilayer nature

provides protection for the inner tubes from chemical reaction with external substances [50].

In the following sections, carbon nanotubes (CNTs) properties, synthesizes, applications and surface modification will be discussed. Moreover, previous studies in using CNTs for heavy metals removal will be reviewed.

1.2.5. Carbon nanotubes. Carbon is the chemical element which has an atomic number 6. It has six electrons occupying 1 s^2, 2 s^2, and $2p^2$ atomic orbital. It can hybridize in sp, sp^2, or sp^3 forms [50]. In the sp^2 hybridization, carbon has the ability to bond in different ways forming amazing structures with completely different properties [50, 51]. A unique cylindrical carbon structures called carbon nanotubes (CNTs) were firstly observed in 1991 [51]. Carbon nanotubes can be visualized as a graphene sheet rolled up in a cylindrical shape [50]. This unique tubular structure has a nanometer diameter and large diameter/length ratio [51]. There are two types of carbon nanotubes (CNTs): single walled carbon nanotubes (SWCNTs) and multi walled carbon nanotubes (MWCNTs) [52]. Figure 1.1 displays a schematic structure for both types. MWCNTs consist of up to several tens graphitic layers with interlayer spacing ranges between 0.34 to 0.39 nm [50, 51]. This multilayer nature provides protection for the inner nanotubes from chemical reactions with external substances as well as higher tensile strength properties compared to SWCNTs. Table 1.2 provides a brief comparison between SWCNTs and MWCNTs. Depending on the number of shells, the outer diameter of MWCNTs ranges from 2 to 30 nm and the inner diameter ranges from 0.4 nm up to several nanometers. According to the way of wrapping in cylindrical shape, SWCNTs can be divided into three forms: armchair, chiral, and zigzag. On the other hand, MWCNTs have two structural forms. The first form is called Russian Doll model. This form contains two carbon nanotubes one inside each other and the outer have a larger diameter than the inner. The second structural form of MWCNTs is called Parchment model and it consists of a single graphene sheet rolled up around itself many times [50].

First ever-obtained CNTs high-resolution transmission electron microscopy (HRTEM) images were in the mid-1970s by Endo when he was studying the internal structure of carbon fibers produced by pyrolysis of benzene and ferrocene.

This discovery did not cause a great impact because - at that time- research was focused on carbon fibers of micron-size. In 1991, Iijima confirmed the existence of helical carbon structures in the soot of arc-discharge reactor [51, 52]. Two years later, SWCNTs were synthesized by adding metal catalysts to the arc-discharge method [51]. Nowadays, there is wide variety of processes to produce CNTs and the worldwide production has increased 10-fold since 2006. Substantially, CNTs-related commercial activity, issued patents and journal publications have also grown [52, 53].

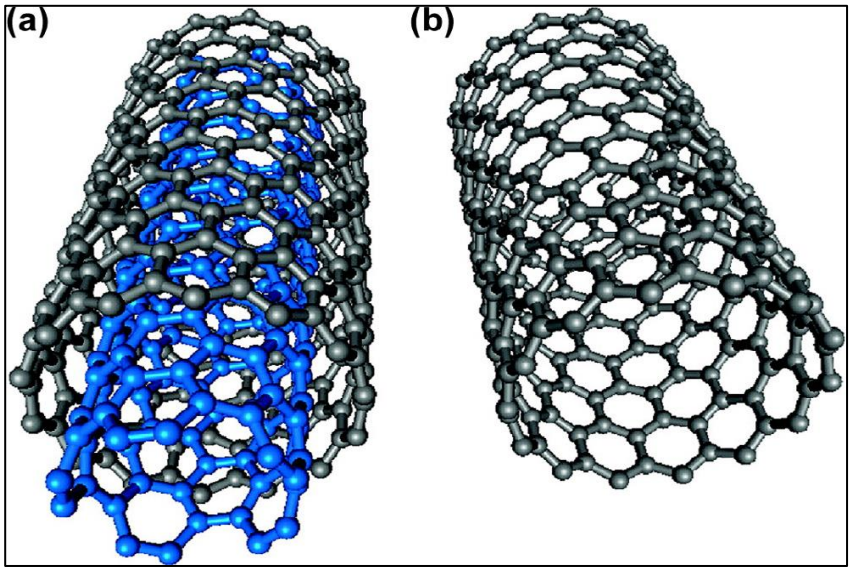

Figure 1.1: Schematic structure of (a) MWCNT and (b) SWCNT [7].

Table 1.2: Comparison between SWCNTs and MWCNTs [50].

SWCNT	MWCNT
Single layer of graphene	Multiple layers of graphene
Low purity	High purity
Simple structure	Very complex structure
More chance of defect during functionalization	Less chance of defect during functionalization
Catalyst is required to synthesize it	No need for catalyst

1.2.5.1. ***CNTs synthesize.*** The increasing industrial applications of CNTs required the development of methods to produce CNTs in large scale. There are three

main techniques used in CNTs production: (1) the electric arc discharge method, (2) the laser ablation method, (3) the chemical vapor deposition [51].

1.2.5.1.1. *Electric arc discharge method.* This method involves the passage of large current (80–100 A) between two opposing high-purity graphite electrodes (6–10 mm OD) separated by an inert gas such as helium (500 torr). During arcing, carbon molecules evaporate from the anode (positive electrode) and solidify on the cathode (negative electrode) in the form of carbon nanotubes at a rate of 1 mm/min [52, 54]. When no catalyst is used in the process, the carbon deposit is MWCNTs. However, a metallic catalyst (such as iron, nickel, and/or cobalt) in needed to synthesize SWCNTs and in this case a purification is required for the final product. CNTs produced using this method is of high quality with less structural defects compared to other methods. This is due to the high temperature used (above 1700 ℃). On the other hand, the little control on the alignment of the produced CNTs is considered as a main disadvantage of this method [50].

1.2.5.1.2. *Laser ablation method.* In this technique, a high-power laser pulses are applied to a quartz tube containing a block of graphite placed inside a furnace at 1200℃ in an atmosphere of inert gas. The laser is used to vaporize the graphite in the tube and the inert gas is maintained within the chamber in order to carry the produced CNTs to the colder area of the chamber from which they are collected [50,54]. Same as in arc discharge method, metallic catalyst particles (usually cobalt or nickel) are essential to synthesize SWCNTs. Properties of the CNTs produced by laser ablation method are affected by the flow and pressure of the inert gas, ambient temperature, the chamber pressure, chemical composition of the target material and the laser properties. The main advantage of this method is the relatively high yield with low impurities. Regardless, quantity of CNTs synthesized per day using this method is less than arc discharge technique. Disadvantages of laser ablation include the non-uniformity of the produced CNTs and the high costs involved because of the need for laser power and high-purity graphite [50].

1.2.5.1.3. *Chemical vapor deposition method (CVD).* In this method, hydrocarbons such as methane or acetylene are thermally decomposed at temperatures ranging from 500 – 1000 ℃ over a catalyst containing transition metal

nanoparticles such as Fe, Ni or Co. When the system is cooled the CNTs grow over the catalyst due to the contact between carbon and metal particles. The catalyst type, purity and porosity affect the yield and structure of the produced nanotubes [50, 51, 54]. The merit of CVD method over electric arc discharge and laser ablation methods is the very well aligned structure of the produced CNTs. Moreover, methane CVD is a promising process for large scale production of CNTs [50, 54].

1.2.5.2. ***CNTs properties and applications*****.** CNTs have unique mechanical, thermal and electrical properties. Mechanically, they are considered as one of the strongest materials [55]. Their tensile strength ranges from 11 to 63 GPa [56]. Moreover, CNTs are characterized by their elasticity. They have the ability to bend and twist and finally return to their original state when the force is removed [57]. CNTs elasticity is determined by the elasticity modules which range from 270 to 950 GPa [56]. On the other hand, CNTs have remarkable thermal properties. MWCNTs have high thermal conductivity reach 3,000 W/K at room temperature [58]. Nanotube composite materials which consist of raw or functionalized CNTs along with other material have higher thermal conductivity; this makes composite materials useful in some industrial applications where high thermal conductivity is required [55]. Besides, CNTs exhibits excellent electrical properties. They are perfect one-dimensional conductors which make them attractable for the fabrication of nano-scale electronic devices [51].

The exceptional properties of carbon nanotubes made them perfect for many applications. Medical, environmental, energy storage and electronic applications are examples of CNTs applications. Medically, nanotubes can be exploited in the fields of tissue engineering, artificial implant, drug delivery and cancer cell identification [50]. Potential applications of CNTs also include: electronic devises, field emission sources, lithium ion batteries and electrochemical devices. Also, they can be used in devising chemical sensors to monitor leaks in plants [52]. They can also be attached to scanning probe microscope tips in order to give better image resolution [57]. In addition, CNTs showed promising results in the field of fillers and coating materials. Addition of CNTs to other materials improves their properties. For example, paints which contain MWCNTs can help reducing ships biofouling. Also, adding nanotubes to metals anticorrosion coatings can increase their stiffness and strength [53, 55].

Gas and energy storage is also one of carbon nanotubes potential applications. The cylindrical, porous and hollow structure of this material makes it ideal for the storage of different chemical species with growing interest in hydrogen because of its usage in fuel-cell-powered vehicles [54, 55]. Moreover, CNTs are also used in water treatment. Portable water filters with CNTs meshes have been developed recently [53]. Furthermore, many studies proved the efficiency of using CNTs as adsorbents for the removal of heavy metals from waste water [7].

1.2.5.3. ***CNTs functionilization.*** Many applications of the carbon nanotubes require handling in aqueous environments. One of the main problems of carbon nanotubes is their tendency to agglomerate and form bundles with each other in aqueous solutions due to Van der Waals forces. This can cause difficulties in CNTs dispersion property. However, this problem can be solved by applying modifications to the surface of the nanotubes. CNTs functionalization or surface modification reduces their accumulation and consequently enhance their dispersion in different mediums and solvents. Moreover, it increases adsorption capacity as well as interaction of CNTs with pollutants [7, 59].

Surface modification can be done using one of two main methods. Covalent method can be used to attach the desired functional group permanently to the surface of nanotubes. In this method, groups are chemically bounded to the surface which can cause defects in the structure of the CNTs and eventually affecting their original properties. Moreover, large amounts of chemicals are used in this method which may cause another environmental problem. Another method for functionalization is the non-covalent method in which functional groups are physically bounded to the surface. This method is important and quite common because it doesn't cause any damage to the structure and properties of the CNTs. Some examples for non-covalent functionalization include wrapping of polymer chains around the nanotubes and adsorption of surfactants on the surface. Surfactants get adsorbed on the surface of the raw carbon nanotubes through their hydrophobic chains making nanotubes hydrophilic and dispersible in aqueous solutions. It is also widely acknowledged that the benzene ring P-stacking interactions onto CNTs surface cause the increase in dispersion in the case of surfactants containing benzene ring [55, 59, 60].

1.2.6. Using CNTs for the removal of heavy metals from wastewater. Recently, using carbon nanotubes for the removal of heavy metals from wastewater have been an attractable issue for researchers and many scientific papers have been published in this issue. Table 1.3 provides summary for the results of selected studies on using carbon nanotubes for the removal of heavy metals from water. In the majority of these studies a functional group was added and its effect on the adsorption behavior was studied. The optimum values of some important parameters such as pH, adsorbent dose and contact time were determined. The optimal solution pH was found to be between 5 and 6 in most of the reviewed papers with few exceptions. However, the optimal contact time was always in the range of 5-120 min. The adsorption capacity differed from one study to another depending on the used functional group.

Wang et al. [61] used magnetic hydroxypropyl chitosan/oxidized multiwalled carbon nanotubes (MHC/OMCNTs) composites as an adsorbent and studied its adsorption characteristics on lead ions in aqueous solutions. The results of this study indicated that the maximum adsorption capacity is 101.1 mg/g. Moreover, Sips model was in good agreement with the experimental data of Wang et al. Thermodynamics study indicated that the adsorption process is endothermic and spontaneous.

Li et al. [62] conducted individual and competitive adsorption experiments on Pb^{+2}, Cu^{+2} and Cd^{+2} in which nitric acid treated MWCNTs were used. Individual adsorption results showed that order of the adsorption capacities is Pb^{+2}> Cu^{+2} > Cd^{+2}. Also, when competitive adsorption is conducted, the order of affinities of CNTs on the three metals followed the same order above. These results are similar to those obtained by Vukovic et al. [63] using ethylenediamine and diethylenetriamine modified MWCNTs; where the adsorption affinity of Pb^{+2} was found to be greater than Cd^{+2}. In another study, pristine MWCNTs was tested by Salam et al. [64] in a competitive adsorption and the results showed this affinity order Cu^{+2}> Zn^{+2}>Pb^{+2}> Cd^{+2} in which the affinity of Pb^{+2} is again greater than Cd^{+2}. Salam et al. [64] also conducted kinetic study which revealed that pseudo second order and Elovich model are the best in describing the experimental data.

Table 1.3: Summary for studies on heavy metals removal using MWCNTs.

Heavy Metal	Diameter (nm)	Functional Group	Adsorption Capacity (mg/g) & Removal%	pH	Contact time (min)	Ref
Pb	80	Magnetic hydroxypropyl chitosan	101.1	5	120	[61]
Pb	20–30	nitric acid	82	5	NA	[62]
Cd			9.2			
Cu			29			
Pb	30	concentrated nitric acid solution	91	5.03	NA	[67]
Pb	5–10	NA	5.21	6.2	NA	[63]
Pb		Oxygen containing	40.79			
Pb		ethylenediamine	44.19			
Pb		diethylenetriamine	58.26			
Pb		triethylenetetramine	NA			
Pb	10 - 30	NA	33	6	60	[69]
Pb		titanium dioxide (TiO_2)	137			
Pb	10 - 20	tris(2- aminoethyl) amine	43	5.7-6	45	[70]
Cu	40- 60	NA	Removal% 84.98	7	120	[64]
Pb			Removal% 31.07			
Cd			Removal% 13.86			
Zn			Removal% 81.69			
Pb	10–20	NA	7.2	5.5	60	[71]
Pb		1-isatin-3-thiosemicarbazone	14.56			
Hg	NA	Thiol	65.52	6.5	NA	[72]
Pb			65.40			
Pb	10–30	NA	Removal% 17	4.1	NA	[66]
Pb	10–30	SDBS	Removal% 80	4.1	NA	[66]
Pb	10–30	TX-100	Removal% 22	4.1	NA	[66]
Pb	10–30	BKC	Removal% 13	4.1	NA	[66]
Pb	110-170	Manganese Oxide (MnO_2)	Removal% 97.3	7-9	5	[65]
Pb	5-10	Oxidized with HNO_3	2.96	9	NA	[73]
Cu			3.49			
Co			2.6			
Pb	< 30	Concentrated nitric acid	85	NA	20	[68]

Manganese oxide (MnO_2) was used as a functional group on MWCNTs in another study [65]. The removal percentage of lead from real sample reached 97.3%. Moreover, when a 10 mg of MWCNTs/MnO_2 was tested on 10 mg/L lead solution of pH 6; the equilibrium removal percentage was 99.8% compared to 56.7% using pristine MWCNTs under same conditions. However, the adsorption capacity of the MWCNTs/MnO_2 was found to be 19.97 mg/g. Zhao et al [69] compared removal of lead using raw MWCNTs to ones modified by titanium dioxide (TiO_2). The results showed a great increase in the adsorption capacity by more than four times. Nonetheless, the effect of nitric acid on the removal of Pb was studied in three different papers [62, 67, 68]. The experiments in the three studies conducted at the same solution pH which is 5, however, the adsorption capacities were found to be 82, 91 and 85 mg/g respectively.

On the other hand, the effect of the presence of surfactants on lead adsorption and the effect of lead on surfactants adsorption using oxidized MWCNTs were studied by Chen et al [66]. In this study, both surfactant and lead solutions were added to the MWCNTs and sonicated for 0.5 hr and shaken for 2 days. Sodium dodecyl benzene sulfonate (SDBS) enhanced the adsorption of lead on MWCNTs; it increased the removal percentage from 17 to 80% when its concentration was increased to 2 mmol/L, however, removal percentage of lead decreased to 45% when the SDBS concentration was further increased to 4 mmol/L. Increasing octyl-phenol-ethoxylate (TX-100) concentration increased the lead removal percentage by only 4%. With regard to the effect of lead concentration on surfactants removal, it was found that increasing lead concentration resulted in doubling the adsorption percentage of the SDBS and increasing TX-100 removal percentage from 38 to 47%. Nevertheless, increasing denzalkonium chloride (BKC) concentration from 0 to 2 mmol/L decreased lead adsorption efficiency from 17 to 13%, BKC adsorption percentage decreased as well when lead concentration increased from 0 to 10.8 mmol/L.

1.3. Thesis Organization

This thesis is divided into four chapters. In chapter 1, background about the importance of removing heavy metals from wastewater and the research objectives

are presented. Moreover, detailed literature review on different techniques used for the removal of heavy metals, adsorption, adsorbents, carbon nanotubes and previous studies in which carbon nanotubes used for the removal of different heavy metals was discussed. Chapter 2 details the materials and instrumentations used in the experimental work. Furthermore, the procedures and methods of the experiments are described in this chapter. Results and discussion are given in chapter 3. Conclusions and recommendations for future work are presented in the fourth chapter.

Chapter 2. Experimental Work

2.1. Materials

Multiwalled carbon nanotubes (>95% purity) were obtained from Grafen Chemical Industries Co (KNT-M31, Turkey) with less than 8 nm diameter and 10-30 microns length. All chemicals used in the experiments were of analytical grade. Double distilled water was used in all experiments. Lead nitrate was obtained from Pharmacos LTD (13353A, England). 1.0 M nitric acid (HNO_3) and 1.0 M sodium hydroxide (NaOH) were used for pH adjustment. Sodium lauryl sulfate (SLS) was provided by DAEJUNG Chemicals & Metals Co., LTD (South Korea). Ferrous sulfate heptahydrate ($FeSO_4.7H_2O$) obtained from Fluka (44980, Germany) and ferric chloride hexahydrate ($FeCl_3.6H_2O$) obtained from Panreac (144358, Spain) were used without any further purification to prepare magnetite nanotubes. 0.7 M nitric acid (HNO_3) was used for adsorbent regeneration.

2.2. Instrumentations

Double distilled water was generated using Water Still Aquatron A4000D (UK). Samples were shaken in a temperature controlled flask shaker (Edmund Buhler, Germany). Syringe filters of 0.45 μm were used (MCE Membrane, membrane solutions, USA). pH measurements were conducted on Basic pH Orion $210A^+$ (ThermoElectron Corporation, USA). Inductively coupled plasma optical emission spectrometry (Varian sequential ICP-OES, USA) and atomic absorption spectrometer (SpectraAA 220FS Varian spectrometer, USA) were used to measure lead concentration. Ultrasonication bath (Elma, Germany) was used to obtain surfactant-coated MWCNTs. Modified adsorbent was centrifuged in centrifuge (HERMLE Labortechnik GmbH, Germany). Hot box oven with fan (GALLENKAMP, UK) and vacuum oven (Wisd Laboratory Instruments, Ireland) were used for drying. MWCNTs were characterized using energy dispersive X-ray spectroscopy EDS detector (Oxford instruments, UK), thermogravimetric analyzer (TGA) (PerkinElmer, USA) and fourier transform infrared spectroscopy (FTIR) (PerkinElmer, USA).

2.3. Methods

2.3.1. Adsorption experiments. The effect of adsorbent dosage, contact time, pH, temperature and initial metal concentration on the removal efficiency were studied using batch mode adsorption experiments. The effect of each parameter was studied by varying it while keeping the other parameters fixed and observing the change in removal percentages. The removal percentage was calculated using equation 19. After determining the optimum value of any parameter, this value was used in the further experiments.

$$\text{Removal \%} = \frac{Co - Ce}{Co} * 100 \quad (19)$$

Where: C_o and C_e are the initial and equilibrium concentrations, respectively (ppm). To conduct the adsorption experiments, 1000 ppm stock lead solution was prepared and then further diluted to other concentrations. The pH of the samples was adjusted using 1.0 M HNO_3 and 1.0 M NaOH. 10 ml of known concentration lead solution were introduced to erlenmeyer flask. Then a known mass of MWCNTs was added to the samples before placing them in temperature controlled flask shaker at 150 RPM. After shaking for a predetermined time interval, samples were filtered using 0.45 μm syringe filters. Final lead concentration was measured using either ICP or AA. For each experiment, two runs and control were carried out. All the glasswares used in the experiments were cleaned using 15% nitric acid and then washed thoroughly with double distilled water before drying in the oven.

2.3.2. Surface modification. To modify the MWCNTs surface with sodium lauryl sulfate (SLS), 0.5 g of raw MWCNTs were added to 500 ml of 8 mM SLS aqueous solution. Well dispersed SLS-MWCNTs suspension was obtained after ultrasonication at 144 W for 2 hours. After that, the dispersion was centrifuged at 4000 rpm for 15 mins and pellets were obtained. Finally, SLS-modified MWCNTs were obtained after drying the pellets for 2 hours at 110 ℃ in hot box oven followed by vacuum drying for 48 hours at 60 ℃ .

2.3.3. Magnetation. To prepare magnetite carbon nanotubes, 100 ml aqueous solution of the molar ratio1:2 Fe^{+2} and Fe^{+3} was prepared and ultrasonicated for 10 min. Few drops of concentrated HCL was added to it to ensure complete dissolution of iron salts.100 ml of MWCNTs aqueous solution was added to the iron solution to

form 200 ml of MWCNTs-Fe_3O_4 aqueous solution with mass ratio 3:2 The MWCNTs-Fe_3O_4 solution was kept in ultrasonication bath for 10 min and the pH was adjusted to 11 using concentrated ammonia. Then, the MWCNTs-Fe_3O_4 solution was kept in hot bath at 50 ℃ under magnetic stirring for 1 hour. The final solution was left for 2 days. After that, the water was separated and the precipitates were dried for 48 hours at 60 ℃ in vacuum oven [74].

2.3.4. Column Operation. For column operation, the magnetite SLS-MWCNTs was filled in a glass column of 50 cm total length and 1.0 cm internal diameter. The height of the bed was kept at 2.0 cm and it was supported by glass wool. The column was loaded with 100 ppm lead solution, which was allowed to percolate under gravity at a flow rate of 1.0 ml/min. Samples were collected for analysis at different time intervals.

2.3.5. Regeneration. To check the reusability of the magnetite SLS-MWCNTs, regeneration was carried out. Adsorption experiments were done at the optimum conditions, and then the used adsorbent was separated for regeneration. Regeneration was done by treating the used adsorbent with 10 ml of 0.7 M HNO_3. The used adsorbent in the regenerating solution was kept for 30 min in thermostatic shaker at room temperature and 150 RPM. The adsorbed lead ions react with HNO_3 to form $PbNO_3$ which is soluble in water. After desorption, the adsorbent was washed four times with double distilled water to remove HNO_3. After that, it was dried at 60 ℃ in vacuum oven for 24 hours and further used in adsorption-desorption cycles.

Chapter 3. Results and Discussion

3.1. Surface Characterization

Surface characterizations for both raw and modified MWCNTs were conducted using Energy Dispersive Spectrometry (EDS), Thermogravimetric analyzer (TGA) and Fourier Transform Infrared Spectroscopy (FTIR). The EDS, TGA and FTIR results are shown in Figures 3.1 - 3.4.

EDS analysis for the raw nanotubes showed that carbon, aluminum and iron are existed on the surface of the MWCNTs. Figure 3.1 shows that carbon represents 96.5 wt%, while aluminum and iron represents 3.2 and 0.4 wt%, respectively. Existence of trace amounts of Al and Fe can be attributed to metal catalysts used in the synthesis of the MWCNTs. The EDS analysis result of the modified adsorbent is shown in Figure 3.2. Carbon weight percentage on the surface dropped to 80.4% and sodium and sulfur were shown to be existed which confirms that modification was successfully achieved.

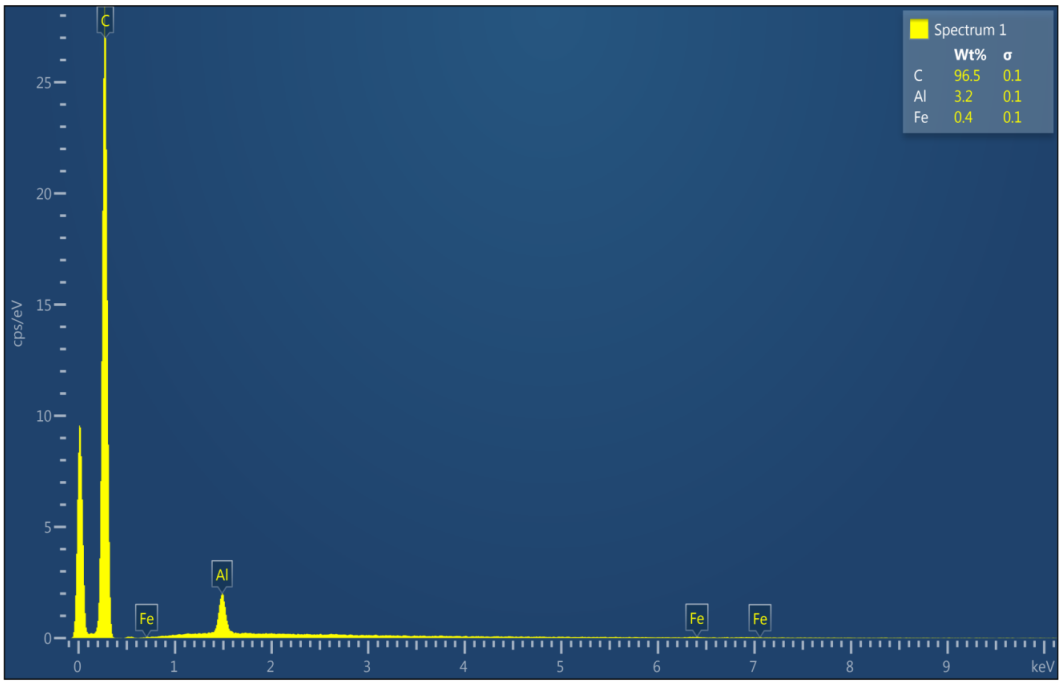

Figure 3.1: Energy Dispersive Spectrometry (EDS) analysis of raw-MWCNTs.

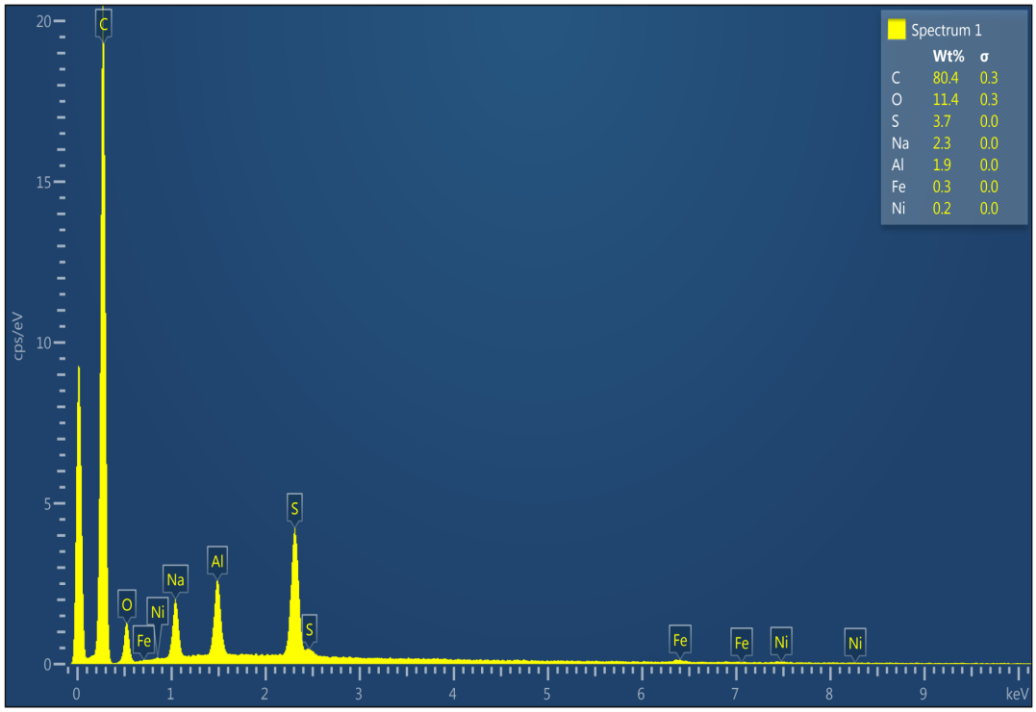

Figure 3.2: Energy Dispersive Spectrometry (EDS) analysis of SLS-MWCNTs.

TGA results also confirmed that the raw MWCNTs have been modified; this is clearly shown in Figure 3.3. The behavior of raw and modified nanotubes with increasing temperatures is totally different. Moreover, it can be concluded from Figure 3.3 that the modified nanotubes are stable with no loss in weight until 200℃. FTIR results for both raw and SLS-MWCNTs are shown in Figure 3.4. Attaching the SLS surfactant to the raw carbon nanotubes resulted in the appearance of more peaks at different wavenumbers. Peaks at 1059.02, 1209.91 and 1374.51 cm^{-1} belong to S=O functional group of sulfurs from the sodium lauryl sulfate [$CH_3(CH_2)_{11}$ SO_4 Na]. Besides, peaks at 2851.64 and 2917.58 cm^{-1} can be attributed to the C-H group of CH_3 and CH_2 and peak at 3406.59 cm^{-1} belongs to the O-H group [75].

It can be concluded that the three characterization techniques used clearly show the difference in the surface of raw and SLS-MWCNTs which confirms that surface modification has been achieved successfully.

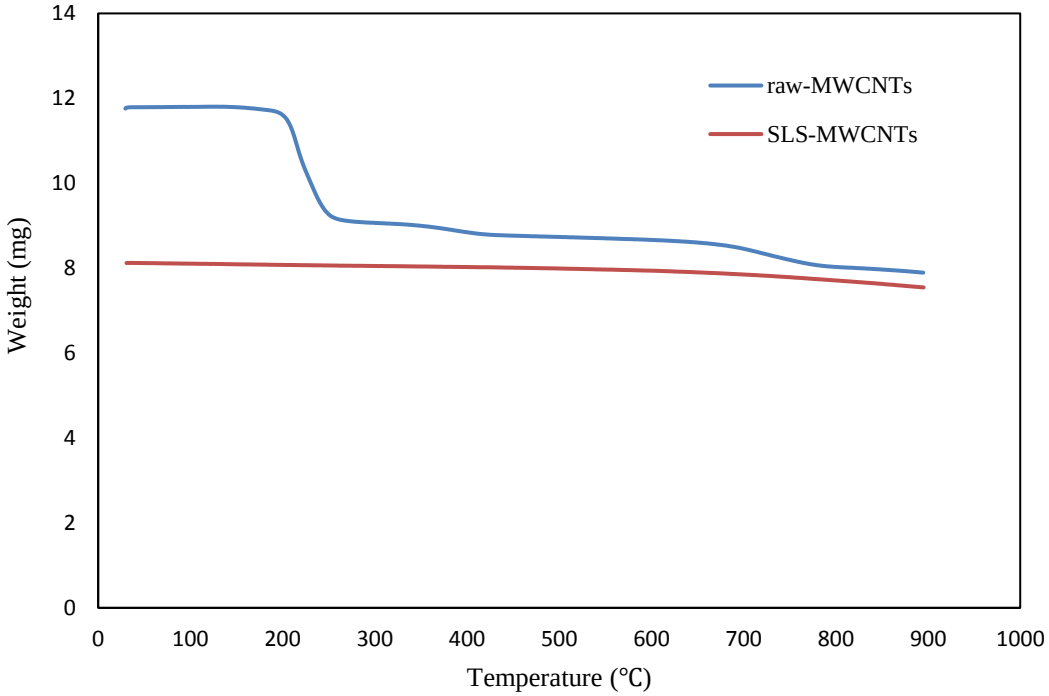

Figure 3.3: TGA results for raw and modified MWCNTs.

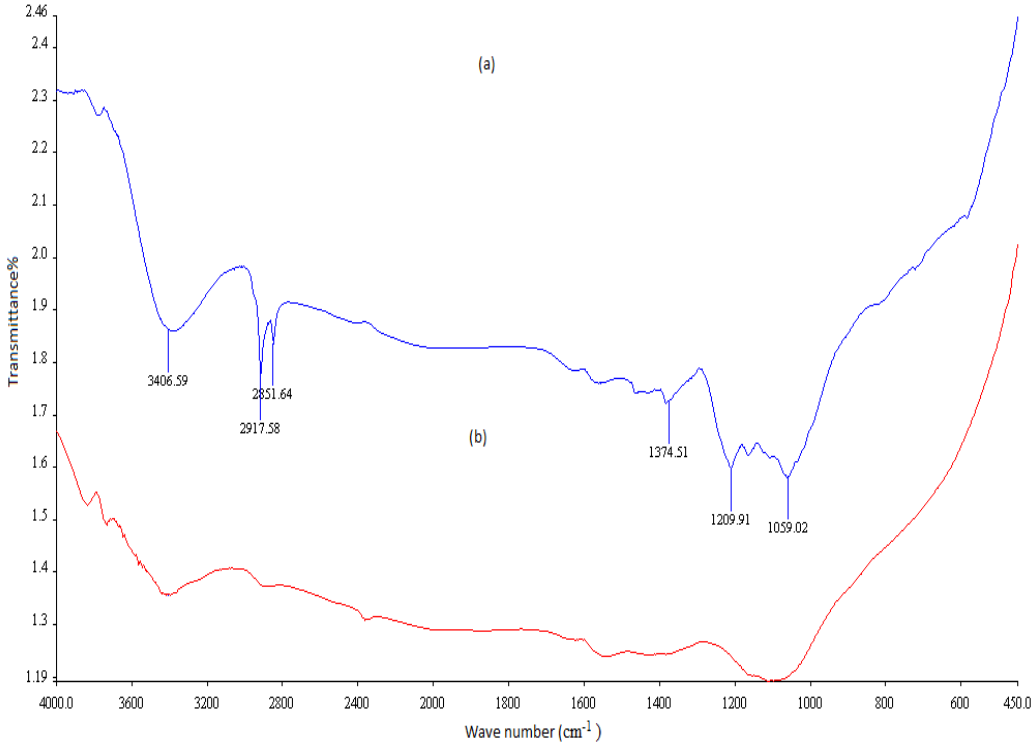

Figure 3.4 : FTIR results for (a) SLS-MWCNTs and (b) Raw-MWCNTs.

3.2. Parameters Optimization

3.2.1. Effect of adsorbent dosage. Adsorbent dosage is a crucial factor which greatly affect the adsorption process; because number of active adsorption sites depend on it. The effect of adsorbent dosage on the removal efficiency using both raw and SLS-MWCNTs was studied and results are shown in Figure 3.5. This was done by using different adsorbent masses per 10 ml lead solution. The dosages were varied in the range between 0.02 to 0.2 g for the raw-MWCNTs and 0.01 to 0.05 g for the SLS-MWCNTs. Other conditions such as initial metal concentration, pH, contact time, temperature and shaking speed were kept constant at 100 ppm, 5.3, 120 min, 25℃ and 150 RPM, respectively. The removal efficiency was noticed to be increasing when the adsorbent mass is increased. This is due to the fact that increasing the amount of adsorbent at constant adsorbate concentration will increase the available active adsorption sites. However, increasing the adsorbent dosage beyond 0.15 g in the case of raw-MWCNTs had no significant change in the removal efficiency. Therefore, 0.15 g was chosen to be the optimum raw-MWCNTs dosage and was used in the further experiments. Salam et al. [64] reported 0.125 g/10 ml optimum dosage for raw-MWCNTs which is very close to the result of this study (0.15 g/ 10 ml).

On the other hand, removal efficiency was noticed to be almost constant using 0.03, 0.04 and 0.05 g of the SLS-MWCNTs. There was less than 2% change in the removal efficiency using these three different dosages. Thus, the optimum dosage of the modified MWCNTs was chosen to be 0.03 g and it gave 95.9% removal efficiency. It is clearly seen from Figure 3.5 that the modified adsorbent achieved much higher removal percentage with much lower dosage. The optimum SLS-MWCNTs dosage is 5 times less than the optimum raw-MWCNTs dosage.

3.2.2. Effect of contact time. Allowing sufficient contact time is important for the adsorption to be achieved. Effect of the contact time on the removal efficiency was studied by changing the contact time starting from 5 min to 120 min while keeping other parameters constant.

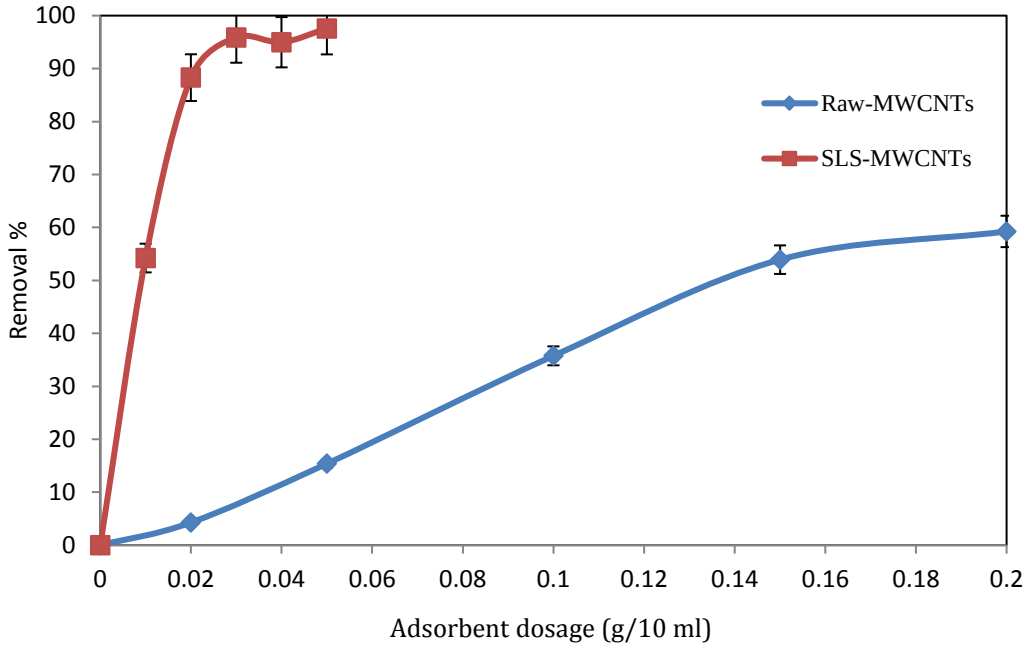

Figure 3.5: Effect of adsorbent dosage on the removal of lead from aqueous solutions for both raw and SLS-MWCNTs at contact time = 120 min, pH = 5.3±0.05, temperature = 25 ± 2 ℃, initial concentration = 100 ppm and shaking rate = 150 RPM.

Optimum dosages of raw and SLS-MWCNTs obtained from previous experiments were used. Results of the effect of contact time on the removal efficiency of lead are presented in Figure 3.6. The figure shows that for both raw and SLS-MWCNTs most of the lead was adsorbed during the first 5 minutes; this can be attributed to the empty active sites available at the beginning. As time moved, adsorption sites get filled with lead and this resulted in low increase in the removal efficiency. Equilibrium for raw-MWCNTs was attained after almost 60 minutes; increasing contact time from 60 min to 120 min resulted in 1% increase in the removal efficiency. Fifty minutes was chosen to be the optimum contact time for the raw-MWCNTs. In the case of SLS-MWCNTs, increasing contact time from 30 min to 120 min changed the removal efficiency from 95.1 % to 95.9 %, respectively. Therefore, 30 min was chosen to be the optimum contact time. In some other studies [60, 65, 68, 69, 70] in which MWCNTs was used with different modifications, it was found that optimum contact time ranges between 5 to 60 min. Thus, it can be concluded that contact time results of this study are in accordance with results reported in literature.

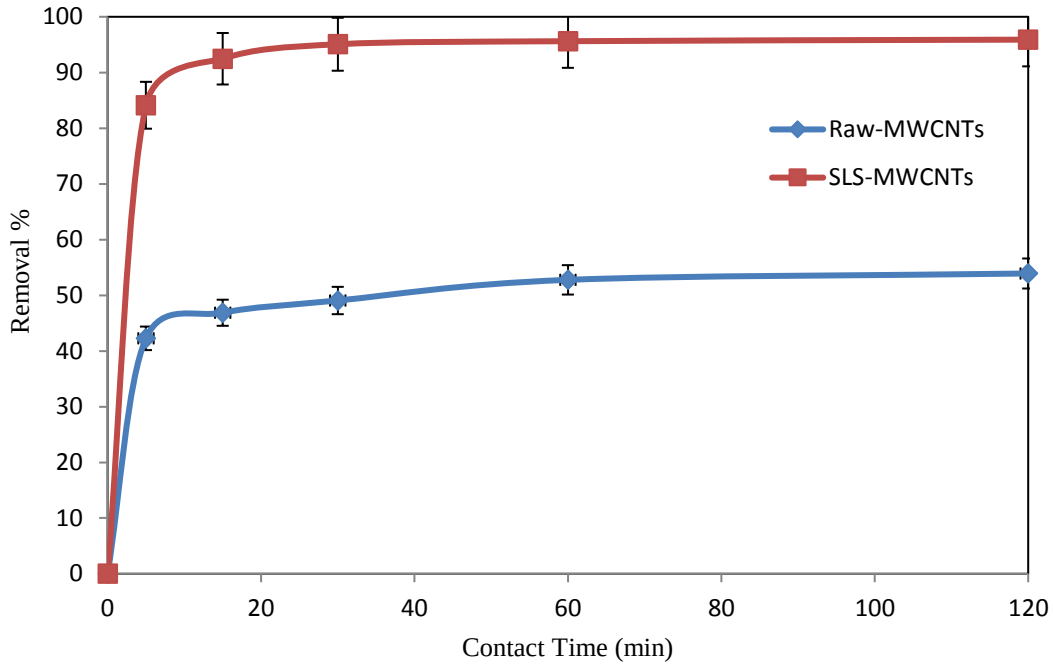

Figure 3.6: Effect of contact time on the removal of lead from aqueous solutions for both raw and SLS-MWCNTs at pH = 5.3±0.05, temperature = 25 ± 2 ℃, initial concentration = 100 ppm and shaking rate = 150 RPM. Adsorbent dosage = 0.15 g/10 ml for raw-MWCNTs and 0.03 g/10 ml for SLS-MWCNTs.

3.2.3. Effect of pH. Solution pH greatly affects the adsorption of lead. This is owning to the fact that lead present in different forms depending on the pH of the solution. The predominant form of lead at pH < 7 is Pb^{+2}. In the pH range from 7 to 10, lead can precipitate in the form of $Pb(OH)_2$ [7]. Thus, at this range it is difficult to claim that lead removal is due to adsorption only. Taking this fact into the account, solutions with different pH starting from 2 to 7 were prepared and the effect of pH on the removal efficiency was studied. Results revealed that as the pH increases, the removal efficiency also increases. This can be due to the competition between hydrogen and lead ions on the available adsorption sites at low pH. As the acidity of the solution decreases, this competition decreases which results in higher removal efficiency. In the case of raw-MWCNTs, there was almost no adsorption at pH 2. Increasing the pH to 4 resulted in 23.3% removal efficiency. Removal percentage continued to increase with increasing pH until it reached 53.9% at 6.5. Optimum pH using raw-MWCNTs was 6.5. For SLS-MWCNTs the removal efficiency was noticed to be constant starting for pH 5.3 and further increase in the pH had no effect

on the removal efficiency. Therefore, pH 5.3 was chosen to be the optimum pH of SLS-MWCNTs and it resulted in 95.1% removal compared to 45.8% using raw-MWCNTs at the same pH. Removal percentage as a function of solution pH for both raw and SLS-MWCNTs is shown in Figure 3.7. The trends of both lines are almost the same, however, higher removal percentages were achieved using SLS-MWCNTs. In previous studies [61, 64, 66, 69] in which MWCNTs was used with different modifications, the optimum pH was in the range between 4 to 7. The results of optimum pH of this study are in the same range.

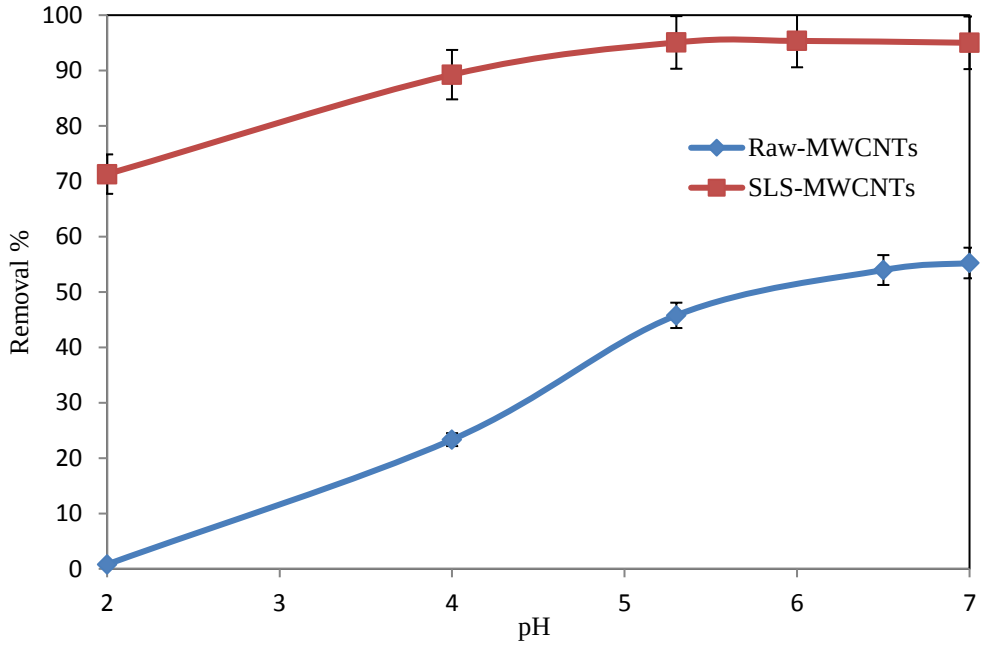

Figure 3.7: Effect of pH on the removal of lead from aqueous solutions for both raw and SLS-MWCNTs at temperature = 25 ± 2 ℃, initial concentration = 100 ppm and shaking rate = 150 RPM. Raw-MWCNTs: adsorbent dosage = 0.15 g/10 ml, contact time = 50 min. SLS-MWCNTs: adsorbent dosage = 0.03 g/10 ml, contact time = 30 min.

3.2.4. Effect of temperature. In order to study the effect of temperature on lead removal, batch adsorption experiments at temperatures ranging from 25 to 45 ℃ were conducted. Figure 3.8 shows the effect of temperature on the removal percentage using raw and SLS-MWCNTs. It can be seen that for the raw-MWCNTs, adsorption of lead slightly increased with the increase of temperature. This endothermic behavior was also reported in previous studies [61, 63]. However, the opposite was noticed in the case of SLS-MWCNTs. Nonetheless, the change in the removal percentage was not found to be very significant for both raw and modified

nanotubes. The change was approximately 6% and 3% using raw and SLS-MWCNTs respectively. Thus, 25 ℃ was chosen to be the optimum temperature and was used in the other experiments.

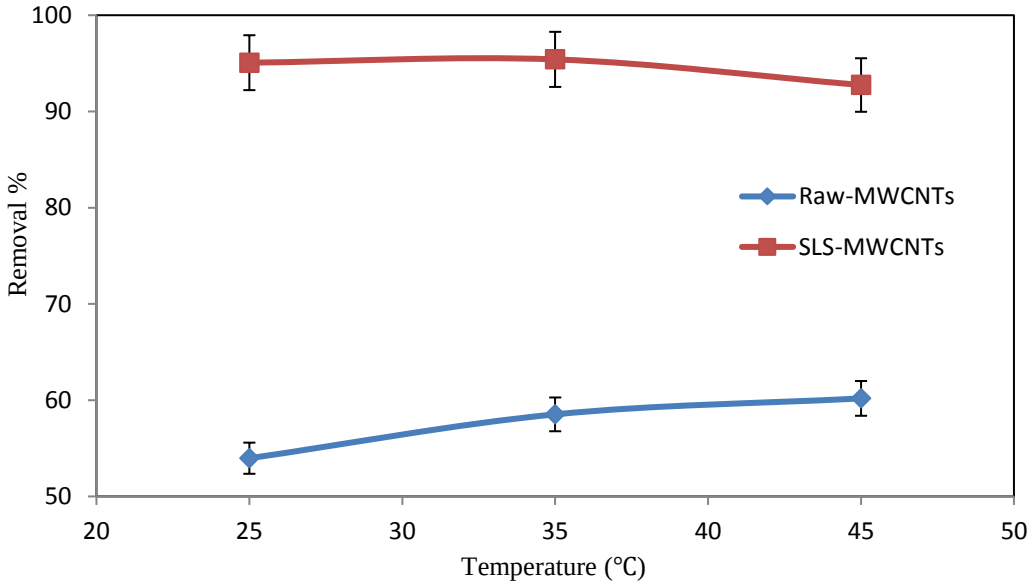

Figure 3.8: Effect of temperature on the removal of lead from aqueous solutions for both raw and SLS-MWCNTs at 100 ppm initial concentration and shaking rate = 150 RPM. Raw-MWCNTs: adsorbent dosage = 0.15 g/10 ml, contact time 50 min, pH = 6.5 ±0.05. SLS-MWCNTs: adsorbent dosage = 0.03 g/10 ml, contact time = 30 min, pH = 5.3 ±0.05.

3.3. Adsorption Equilibrium Isotherms

Studying the adsorption equilibrium is essential to predict the effectiveness of the adsorption process for a given system. Lead solutions with different initial metal concentrations and fixed pH, contact time, temperature and adsorbent dosage were used to study the adsorption equilibrium. Adsorption capacity was calculated using equation (20):

$$q_e = \frac{(Co - Ce) * V}{m} \qquad (20)$$

where: q_e is the equilibrium adsorption capacity (mg/g), C_o and C_e are the initial and equilibrium concentrations, respectively (ppm). V is the volume of solution (ml) and m is the mass of adsorbent (g). Adsorption capacity as function of initial concentration for raw and SLS-MWCNTs is shown in Figures 3.9 and 3.10, respectively. The adsorption capacity of raw-MWCNTs was found to be very low compared to the adsorption capacity of SLS-MWCNTs. The adsorption capacity

using raw-MWCNTs at 100 ppm was found to be 3.70 mg/g compared to 30 mg/g using SLS-MWCNTs at the same concentration. This result shows that the modification has greatly enhanced the adsorption capacity. Moreover, SLS-MWCNTs was able to adsorb lead until 700 ppm with 146 mg/g adsorption capacity.

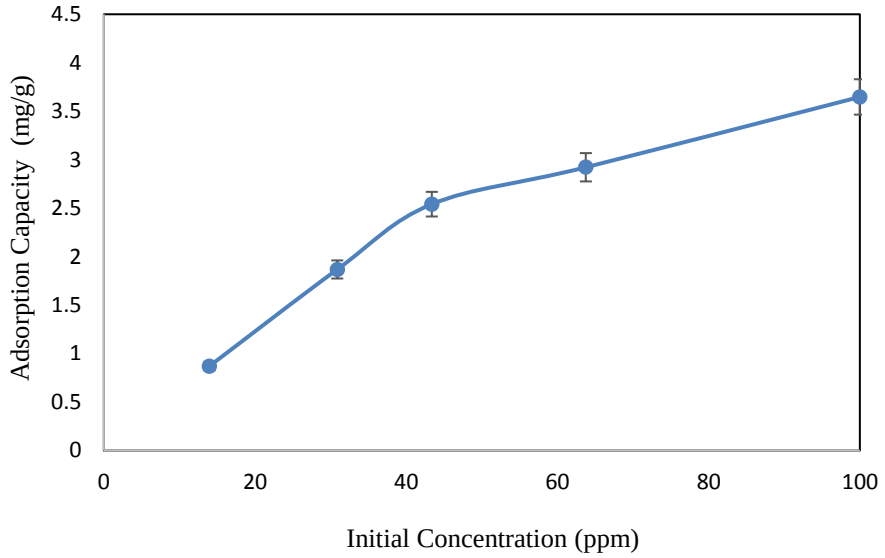

Figure 3.9: Change in adsorption capacity with initial concentration using raw-MWCNTs at adsorbent dosage = 0.15 g/10 ml, contact time = 50 min, pH = 6.5 ±0.05, temperature = 25 ± 2 ℃ and shaking rate = 150 RPM.

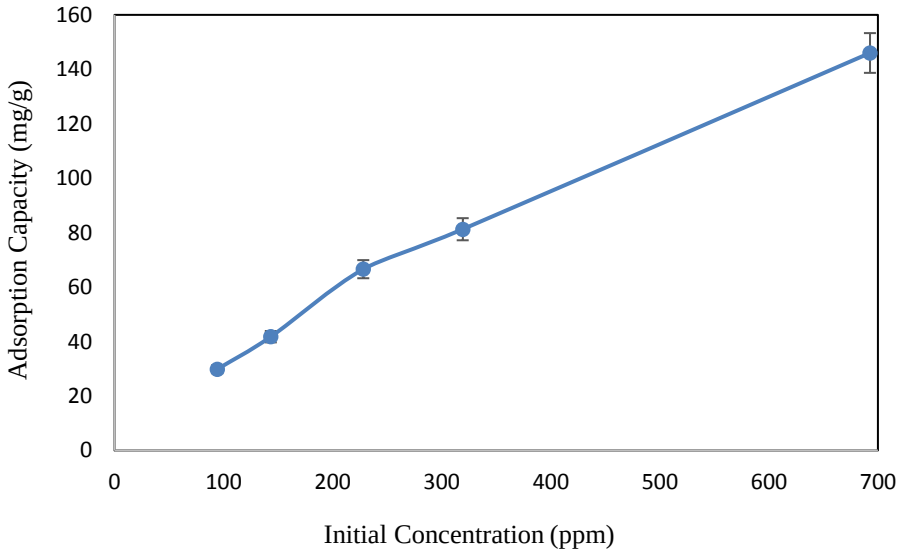

Figure 3.10: Change in adsorption capacity with initial concentration using SLS-MWCNTs at adsorbent dosage = 0.03 g/10 ml, contact time = 30 min, pH = 5.3 ±0.05, temperature = 25 ± 2 ℃ and shaking rate = 150 RPM.

The equilibrium data of raw and SLS-MWCNTs were fitted on different two parameter isotherms models such as Langmuir, Freundlich, Temkin and Dubinin-Radushkevich.

Equations of these models are presented in Section 1.2.3.1. The isotherm model which best describe the adsorption data was determined. The best model is the one which has the highest coefficient of determination (R^2) value. Results of data fitting on isotherm models are shown in Figures A.1 to A.8 in Appendix A. R^2 values as well as models parameters for both raw and SLS-MWCNTs are given in Tables 3.1 and 3.2.

3.3.1. Langmuir isotherm model. The R^2 for the raw-MWCNTs is 0.99 which is the highest compared to other models. This suggests that Langmuir model is the best one in describing adsorption of lead on raw-MWCNTs. The maximum adsorption capacity of the raw-MWCNTs calculated from this model is 3.84 mg/g. Since Langmuir is the best fit for adsorption of lead on raw nanotubes; it can be concluded that the adsorption is monolayer and reversible [33]. For the SLS-MWCNTs, the value of R^2 is 0.96 and it is not the highest amongst the studied model; which means that Langmuir is not the perfect model for lead adsorption using SLS-MWCNTs.

3.3.2. Freundlich isotherm model. This model doesn't perfectly describe lead adsorption on raw-MWCNTs; the R^2 is equal to 0.88. However, it is the best one in the case of SLS-MWCNTs. Its R^2 has the highest value compared to the other studied models. The values of Freundlich parameters for both raw and SLS-MWCNTs are given in Tables 3.1 and 3.2. Results showed that K_F for raw and SLS-MWCNTs are 1.1 and 15 g/mg. K_F is Freundlich indicative of relative adsorption capacity of an adsorbent. Higher value of K_F in the case of SLS-MWCNTs indicates higher adsorption capacity. The adsorption capacity of SLS-MWCNTs was calculated from this model at 700 ppm initial concentration by substituting the values of Freundlich parameters in equation (3). The result is 141 mg/g which is much higher than the maximum adsorption capacity of the raw nanotubes (3.84 mg/g).

3.3.3. Temkin isotherm model. R^2 for both adsorbents are greater than 0.90, however, this model doesn't give the highest value of R^2 when it is compared to the other models. This concludes that Temkin is not the best fit neither for raw nor SLS nanotubes.

3.3.4. Dubinin-Radushkevich isotherm model. D-R model is the worst in describing adsorption of lead on raw and SLS-MWCNTs. Results which are given in Tables 3.1 and 3.2 show that this model give the least values of R^2 compared to the other models. Values of R^2 were found to be 0.53 and 0.89 for raw and SLS-MWCNTs, respectively. This concludes that D-R model is not the best fit neither for raw nor SLS nanotubes.

Table 3.1: Parameters of four adsorption isotherm models for lead removal using raw-MWCNTs.

Adsorption Isotherm Model	Parameters	R^2
Langmuir	q_m = 3.8 mg/g K_L = 0.29 L/mg	0.99
Freundlich	n = 2.90 K_F = 1.10 ($mg^{1-1/n}.L^{1/n}$)/g	0.88
Temkin	A_T = 10.00 L/g B_T = 4200 mol/J	0.94
Dubinin-Radushkevich	q_s = 3.20 mg/g K_{DR} = $1*10^{-6}$ mol^2/kJ^2	0.53

Table 3.2: Parameters of four adsorption isotherm models for lead removal using SLS-MWCNTs.

Adsorption Isotherm Model	Parameters	R^2
Langmuir	q_m = 167 mg/g K_L = 0.021 L/mg	0.96
Freundlich	n = 2.50 K_F = 15.00 ($mg^{1-1/n}.L^{1/n}$)/g	0.97
Temkin	A_T = 0.38 L/g B_T = 86.00 mol/J	0.90
Dubinin-Radushkevich	q_s = 78.00 mol^2/kJ^2 K_{DR} = $4*10^{-6}$ mg/g	0.89

The adsorption capacities of different modified MWCNTs used for the removal of lead from aqueous solutions are shown in Table 3.3. Different functional groups were attached and different adsorption capacities were obtained.

The adsorption capacity of SLS-MWCNTs which is used in this study was calculated from Freundlich model. Freundlich model was found to be the best model in describing the adsorption data of SLS-MWCNTs. The value of the adsorption capacity was found to be 141 mg/g which is the highest compared to the other modified adsorbents shown in Table 3.3. It is followed by TiO_2 modified MWCNTs which has 137 mg/g adsorption capacity.

Table 3.3: Adsorption capacities of different modified MWCNTs used for lead removal from aqueous solutions.

Functional Group	Adsorption Capacity (mg/g)	Reference
Magnetic hydroxypropyl chitosan	101.1	[61]
Nitric acid	82	[62]
2-vinylpyridine (VP)	37	[7]
Oxygen containing	40.79	[63]
Ethylenediamine	44.19	
Diethylenetriamine	58.26	
Titanium dioxide (TiO_2)	137	[69]
tris(2- aminoethyl) amine	43	[70]
1-isatin-3-thiosemicarbazone	14.56	[71]
Thiol	65.40	[72]
Manganese oxide	78.74	[65]
Oxidized with HNO_3	2.96	[73]
Concentrated nitric acid	85	[68]
3-aminopropyltriethoxysilane (APTS)	75.02	[7]
Sodium Lauyrl Sulfate	141	This study

3.4. Adsorption Kinetics

Studying the adsorption kinetics is important in determining the rate at which adsorption process takes place. It is essential for determining the adsorbate residence time and the system design. The results of data fitting on the pseudo- first order model, pseudo- second order model and Elovich model for both raw and SLS-MWCNTs are shown in Figures A.9 to A.14 in appendix A. Equations of the three models are given in Section 1.2.3.2. Tables 3.4 and 3.5 show R^2 values as well as parameters of pseudo- first order model, pseudo- second order model and Elovich model for both raw and SLS-MWCNTs. It can be seen that adsorption contact time data of both raw and SLS-MWCNTs are well fitted by the pseudo- second order model. R^2 values were found to be equal to 1 for both raw and SLS nanotubes. Thus, it can be concluded that the lead ions uptake on the surface of both adsorbents is governed by pseudo- second order rate equation. Same result was reported in previous studies [61, 63, 69] in which MWCNTs was used with different modifications.

Table 3.4: Parameters of three adsorption kinetics models for lead removal using raw-MWCNTs.

Adsorption Kinetics Model	Parameters	R^2
Pseudo- first order	$k_1 = 0.038\ min^{-1}$	0.94
Pseudo- second order	$k_2 = 0.110$ g/ mg.min	1
Elovich	$\alpha = 36000$ mg/g.min $\beta = 4.9$ g/mg	0.95

Table 3.5: Parameters of three adsorption kinetics models for lead removal using SLS-MWCNTs.

Adsorption Kinetics Model	Parameters	R^2
Pseudo- first order	$k_1 = 0.066$ min-1	0.92
Pseudo- second order	$k_2 = 0.055$ g/ mg.min	1
Elovich	$\alpha = 5.00 * 10^9$ mg/g.min $\beta = 0.88$ g/mg	0.81

3.5. Adsorption Mechanism

Adsorption mechanism models are used to determine the controlling step in the adsorption process; either film diffusion or particle diffusion. The slowest step is the limiting step. Intra-particle and liquid film diffusion models are used below in order to study the adsorption mechanism of raw and SLS-MWCNTs. Equations of these two models are given in Section 1.2.3.3. Figures 3.11 and 3.12 shows the results of intra-particle diffusion model for raw and SLS-MWCNTs, respectively. Although, the graphs show some degree of linearity, however, the plots do not pass through the origin which means there are other mechanisms contributing in the controlling step other than the intra-particle diffusion [42]. Moreover, the large value of the intercept in the case of SLS-MWCNTs indicates higher contribution of surface sorption in the limiting step.

On the other hand, the fittings of liquid film diffusion model for raw and SLS-MWCNTs are presented in Figures 3.13 and 3.14. R^2 values are higher than the case of intra-particle diffusion model, but again the plots do not pass through the origin which means that liquid film diffusion is not the limiting step in the adsorption process [44].

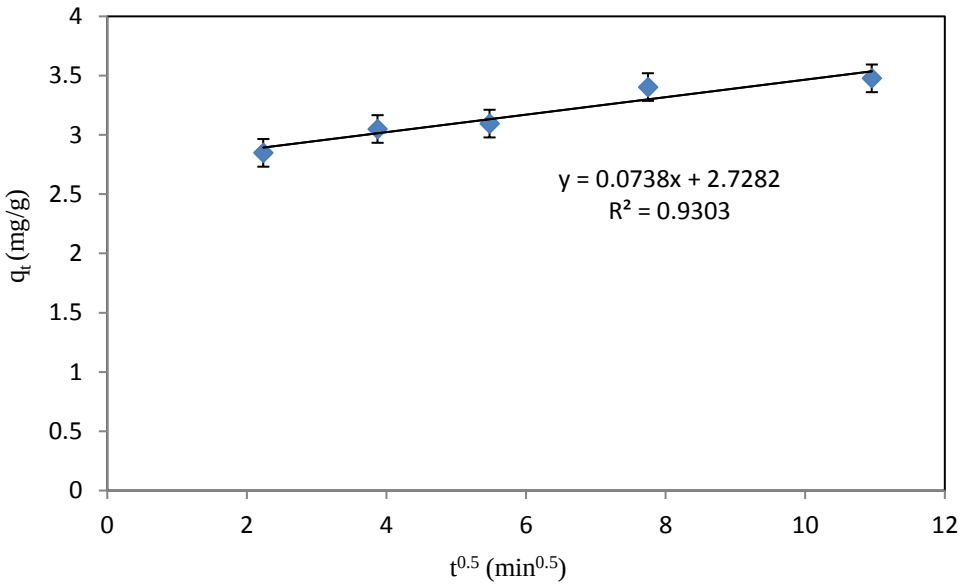

Figure 3.11: Intra-particle diffusion model for lead adsorption using raw-MWCNTs.

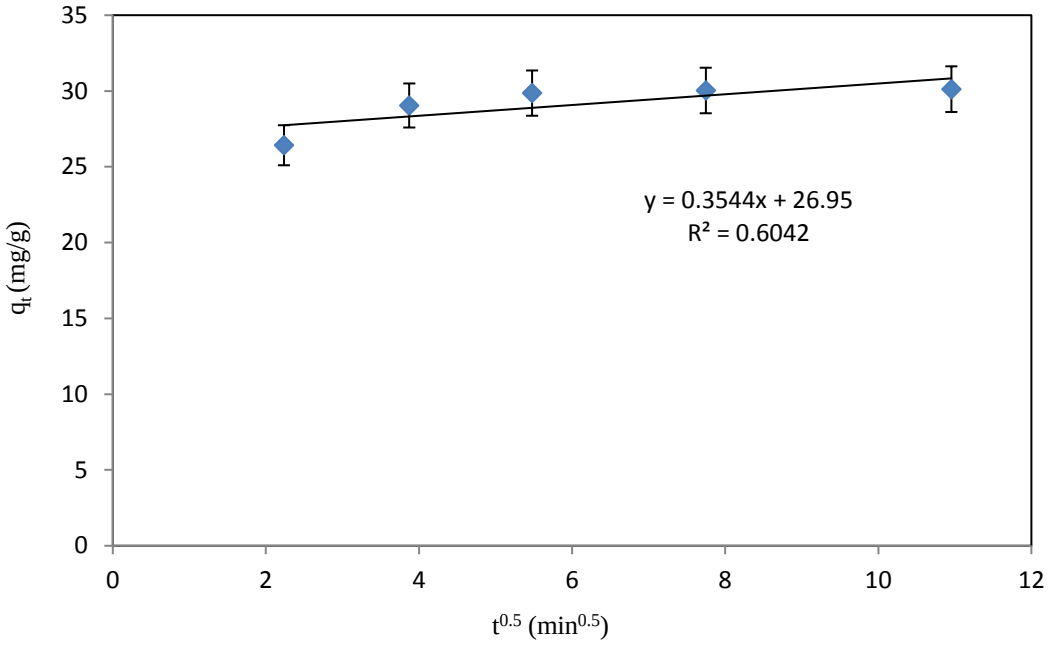

Figure 3.12: Intra-particle diffusion model for lead adsorption using SLS-MWCNTs.

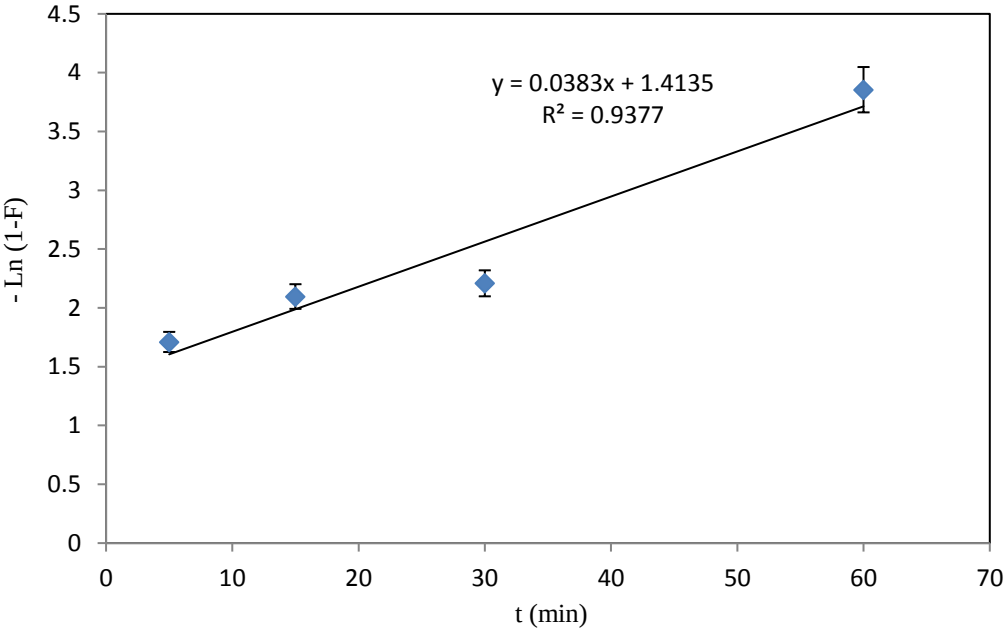

Figure 3.13: Liquid film diffusion model for lead adsorption using raw-MWCNTs.

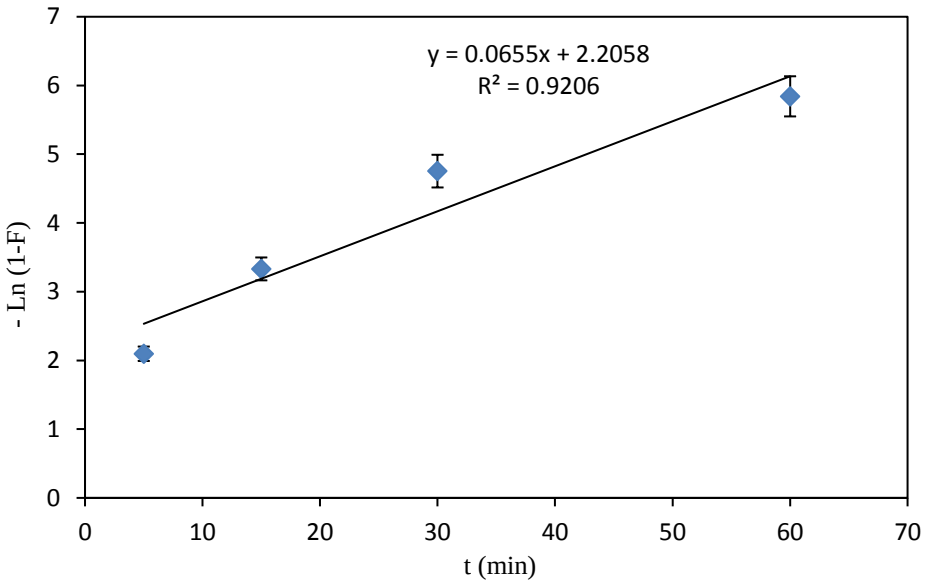

Figure 3.14: Liquid film diffusion model for lead adsorption using SLS-MWCNTs.

3.6. Absorption Thermodynamics

Some thermodynamics parameters such as gibbs free energy change (ΔG), enthalpy change (ΔH) and entropy change (ΔS) are important to fully understand any adsorption process. Values of these three parameters were calculated for lead adsorption on both raw and SLS-MWCNTs. Equations used in calculating the three parameters are given in Section 1.2.3.4. Van't Hoff plots of Ln K_c vs 1/T for raw and SLS-MWCNTs are given in Figures A.15 and A.16 in appendix A. The values of the three parameters are given in Tables 3.6 and 3.7.

The positive value of ΔH when raw MWCNTs are used indicates an endothermic adsorption behavior, however, for SLS-MWCNTs a negative ΔH value was obtained which suggests an exothermic behavior. This difference in behavior can be attributed to some kind of ion exchange involved in the case of raw-MWCNTs. On the other hand, the negative values of ΔG indicates that the adsorption process is spontaneous [46]. Since all ΔG values are between 0 and -20 kJ/mol, it can be concluded that the adsorption process is physisorption [77]. This is the case for both raw and SLS-MWCNTs. The sign of the entropy change gives information about the degree of freedom of the adsorbate. The positive ΔS value of SLS-MWCNTs indicates an increase in the degree of freedom of the lead ions [47].

Table 3.6: Thermodynamics parameters of lead adsorption using raw-MWCNTs.

ΔG (kJ/mol)	25 ℃	-0.45
	35 ℃	-0.79
	45 ℃	-1.10
ΔH (kJ/mol)	9.90	
ΔS (kJ/mol.°K)	0.035	

Table 3.7: Thermodynamics parameters of lead adsorption using SLS-MWCNTs.

ΔG (kJ/mol)	35 ℃	-7.80
	45 ℃	-6.40
	50 ℃	-5.70
ΔH (kJ/mol)	-51.00	
ΔS (kJ/mol.°K)	-0.14	

3.7. Magnetation

The very light weight of carbon nanotubes limits their application in columns; because they can flow out with the fluid. Therefore, it is very important to find a manner to make them denser and consequently stable when they packed in a column. Magnetation is an efficient way to make nanotubes heavier and hence practical for using in adsorption columns. In this work, magnetite pellets of raw MWCNTs were prepared following the procedure described in Section 2.3.4. After that, the magnetite pellets were modified with the SLS to obtain magnetite SLS nanotubes (Mag SLS-MWCNTs). The magnetite adsorbent was characterized using FTIR to make sure that magnetation is achieved and the modification functional groups are still existed. Figure 3.15 shows comparison between raw, raw-magnetite and mag-SLS MWCNTs. The peak at 493.89 cm^{-1} in the raw-magnetite spectra confirms the presence of iron oxide used in preparing the magnetite pellets [78]. The FTIR spectra of mag-SLS MWCNTs shows the groups added by both SLS modification and magnetation.

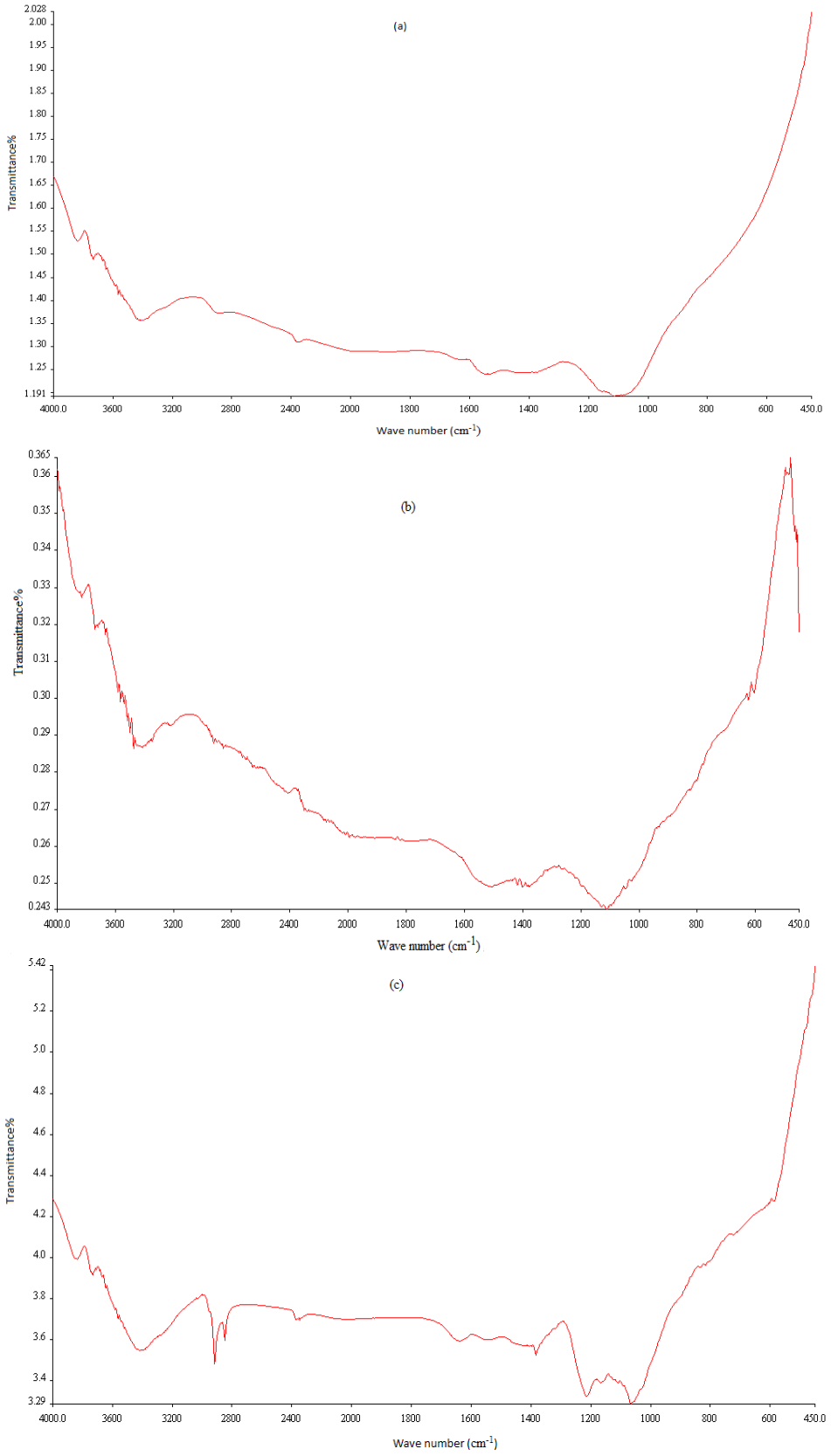

Figure 3.15: FTIR results of: (a) Raw-MWCNTs, (b) Mag-MWCNTs and (c) Mag SLS-MWCNTs.

Before using the magnetite SLS-MWCNTs in column, they were firstly tested in batch experiments to make sure that the magnetation has no effect on the efficiency of the SLS-MWCNTs. Results of magnetite SLS-MWCNTs are shown in Figures 3.16 – 3.19. The graphs show comparison between the magnetite and non-magnetite SLS-MWCNTs. It is clearly seen that the efficiency of both adsorbents is approximately the same. Therefore, it can be concluded that the magnetation has no effect on the efficiency of SLS-MWCNTs and the magnetite SLS-MWCNTs can be used confidently in a column.

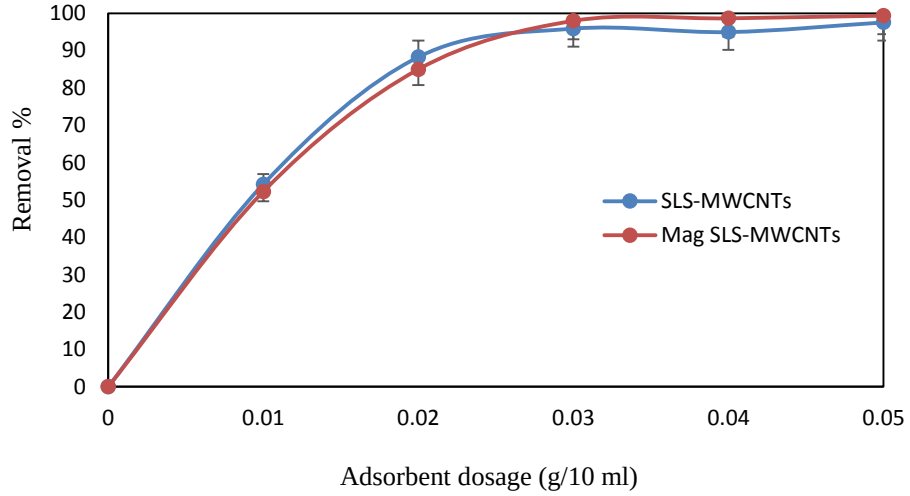

Figure 3.16: Effect of adsorbent dosage on the removal of lead from aqueous solutions for magnetite and non-magnetite SLS-MWCNTs at contact time = 120 min, pH = 5.3±0.05, temperature = 25 ± 2 ℃, initial concentration = 100 ppm and shaking rate = 150 RPM.

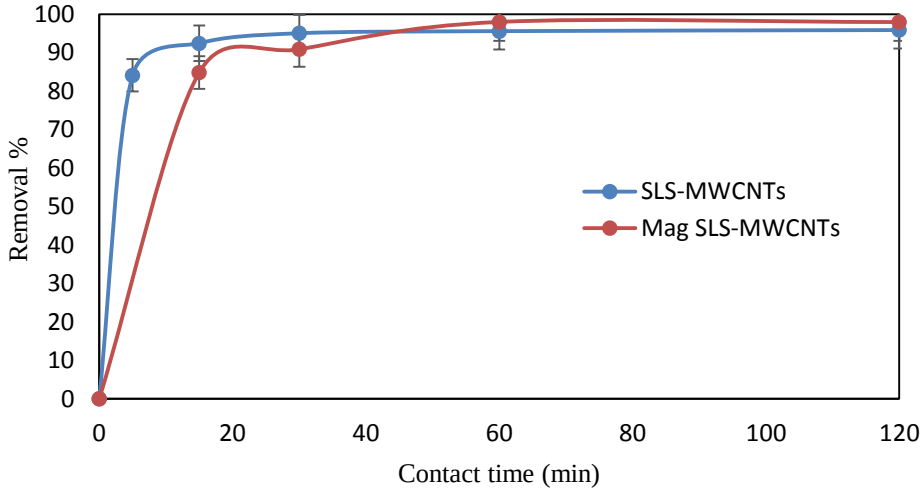

Figure 3.17: Effect of contact time on the removal of lead from aqueous solutions for magnetite and non-magnetite SLS-MWCNTs at adsorbent dosage = 0.03 g/10 ml, pH = 5.3±0.05, temperature = 25 ± 2 ℃, initial concentration = 100 ppm and shaking rate = 150 RPM.

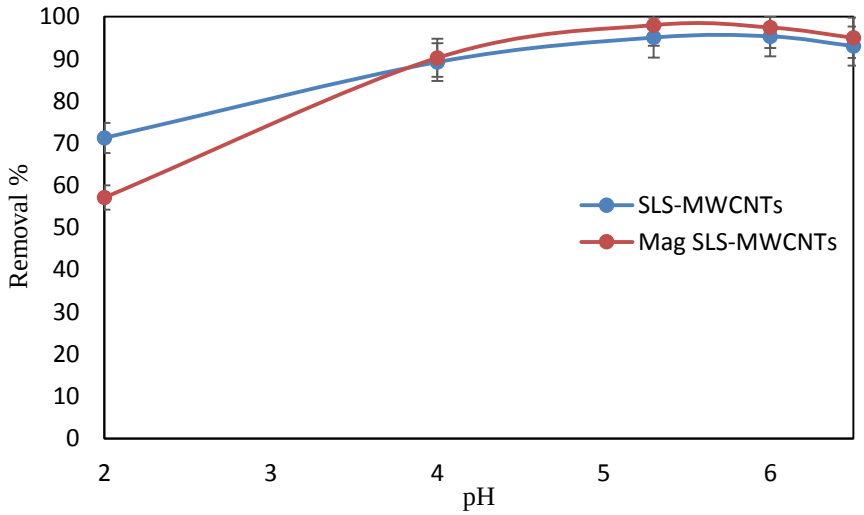

Figure 3.18: Effect of pH on the removal of lead from aqueous solutions for magnetite and non-magnetite SLS-MWCNTs at adsorbent dosage = 0.03 g/10 ml, contact time = 30 min, temperature = 25 ± 2 ℃, initial concentration = 100 ppm and shaking rate = 150 RPM.

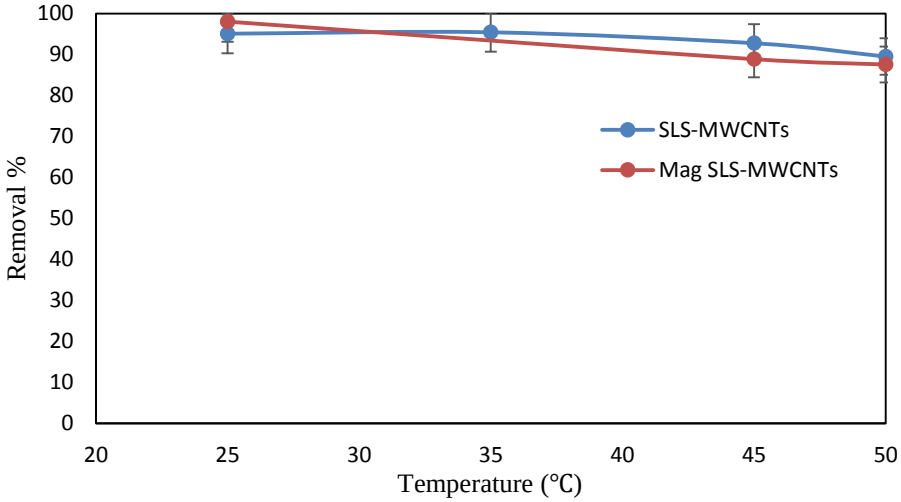

Figure 3.19: Effect of temperature on the removal of lead from aqueous solutions for magnetite and non-magnetite SLS-MWCNTs at, adsorbent dosage = 0.03 g/10 ml, contact time = 30 min, pH = 5.3±0.05, initial concentration = 100 ppm and shaking rate = 150 RPM.

3.8. Column Experiments

The first step in testing the efficiency of any new adsorbent is using it in batch process. However, batch method is not convenient in treating large scale wastewater; fixed bed adsorption columns are used instead. In column operation, the contaminated fluid is continuously fed through bed packed with the adsorbent until the bed is fully loaded with the adsorbate. Column experiments were carried out

following the procedure described in Section 2.3.4. Figure 3.20 shows the results of the column operation expressed in terms of the change in C_t/C_o with time. It can be seen that C_t/C_o increases with time; this is because more volume of the contaminated fluid has passed through the column which makes it exhausted and loaded with the lead.

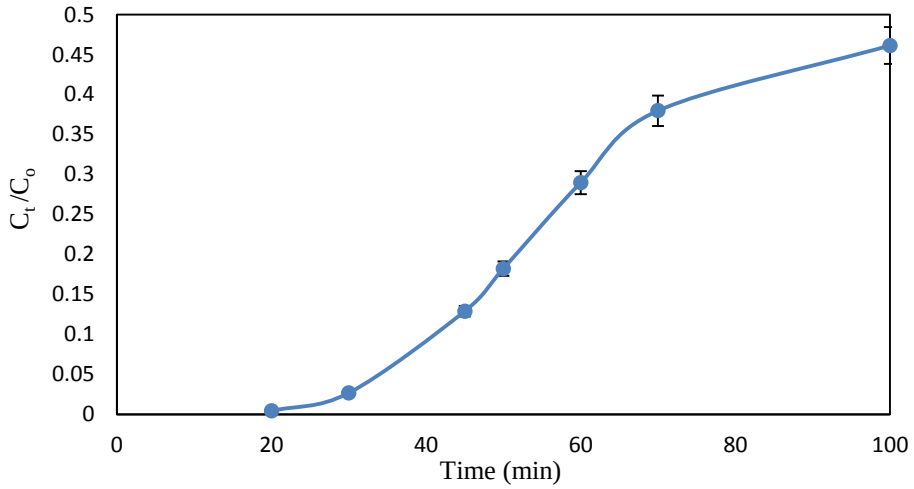

Figure 3.20: Effect of time on C_t/C_o in column operation at initial concentration = 100 ppm, pH = 5.3±0.05 and 2 cm bed height.

3.8.1. Fixed bed column adsorption models. It is very important to predict the performance of fixed bed column under different conditions. Since experimental determination is expensive and time consuming; it is convenient to use mathematical models to determine the operating conditions and to optimize the design of packed bed columns [79]. Below are four models which were used to fit the column experimental data.

3.8.1.1. *Thomas model.* This is a frequently used model to predict the adsorption capacity of adsorbents in columns. Thomas model assumes Langmuir model, second order kinetic reaction and negligible internal and external diffusion resistances [79]. It is expressed by equation (20) [80]:

$$Ln\left[\frac{C_o}{C_t} - 1\right] = \frac{k_{Th}\ q\ m}{Q} - k_{Th}\ C_o\ t \qquad (20)$$

where: C_o and C_t are the initial concentration and concentration at time t (mg/L), respectively, k_{Th} is Thomas kinetic coefficient (ml/min.mg), q is the adsorption capacity (mg/g), m is the mass of adsorbent in the column and Q is the fluid

volumetric flow rate (ml/min). k_{Th} and q_o can be calculated from the slope and intercept of $Ln\,[\,\frac{Co}{Ct} - 1]$ versus t [80].

3.8.1.2. *Yoon–Nelson model.* It is a simple straightforward model applicable for one component system. It requires less column data compared to other models. Yoon-Nelson model can predict the time required for 50% column breakthrough without the need to run column experiments for long time. However, it is not suitable in predicting process variables [79, 80]. Yoon-Nelson model is given in equation (21) [80]:

$$Ln\,[\,\frac{C_t}{C_o - C_t}\,] = k_{YN}\,t - \tau\,k_{YN} \qquad (21)$$

where: k_{YN} is Yoon-Nelson rate constant (min^{-1}) and τ is time required for 50% column breakthrough (min). k_{Th} and τ can be found from plot of $Ln\,[C_t / (C_o - C_t)]$ versus t [80].

3.8.1.3. *Adam–Bohart model.* This model is based on surface reaction theory and assumes that the reaction is not immediate. It is convenient in describing the initial part of column operation. Adam-Bahart model is expressed by equation (22) [80]:

$$Ln\,[\,\frac{C_t}{C_o}\,] = k_{AB}\,C_o\,t - \frac{k_{AB}\,N_o\,z}{U_o} \qquad (22)$$

where: k_{AB} is Adam-Bohart kinetic constant (L/mg.min), N_o is the saturation concentration (mg/L), z is the height of bed (cm) and U_o is the velocity calculated from the volumetric flow rate over the column cross section area (cm/min). k_{AB} and N_o can be found by plotting $Ln\,[C_t / C_o]$ versus t [80].

3.8.1.4. *Modified dose response model (MDR).* This model was developed originally for pharmacology studies and recently it has been used to describe adsorption of metals [79]. Compared to Thomas model, the MDR model is more accurate in predictions at low and high time intervals of the breakthrough curve [81]. The MDR model is expressed by equation (23) [79]:

$$Ln\left[\frac{C_t}{C_o - C_t}\right] = a' Ln\,(C_o * Q * t) - a' Ln\,(q * m) \qquad (23)$$

where: a' is the MDR model constant and it can be found by plotting $Ln\left[\frac{C_t}{C_o - C_t}\right]$ versus $Ln\,(Co*Q*t)$.

The experimental data collected from column operation were fitted in the previous four models and results are shown in Figures A.17 - A.20 in appendix A. Column experiments were done at the following conditions: height of the column (z) was 2.0 cm, the volumetric flow rate (Q) was 1.0 ml/min, the initial concentration (C_o) was 100 ppm and the velocity (U_o) was 1.27 cm/min. These data as well as the slopes and intercepts of experimental data fitting were used to calculate the parameters of the four models. From results given in Table 3.8, it can be seen that the MDR model is the best one in describing the column's data with R^2 = 0.95. By replacing the MDR parameters in equation (23), it can be predicted that column will reach 90% exhaustion after 160 min.

Table 3.8: Fixed bed column models parameters.

Model	Parameters	R^2
Thomas	q (mg/g) = 28.00 k_{Th} (ml/mg.min) = 0.64	0.79
Yoon–Nelson	τ (min) = 85.00 k_{YN} (min^{-1}) = 0.06	0.79
Adam–Bohart	N_o (mg/L) = 6033 k_{AB} (ml/mg.min) = 0.55	0.73
MDR	q (mg/g) = 28.00 a' (1/mg) = 3.50	0.95

3.9. Regeneration

Regeneration was done for the magnetite SLS-MWCNTs using the procedure described in Section 2.3.5. The results of two cycles are shown in Figure 3.21. Removal percentage dropped from 97.04% to 59.06% and from 59.06% to 33.59%. It can be concluded that regenerating magnetite SLS-MWCNTs using 0.7 M HNO_3 for 30 min is not very efficient. Therefore, it is recommended to find more efficient

method for regeneration such as KCl or higher concentration of nitric acid coupled with heating cycle.

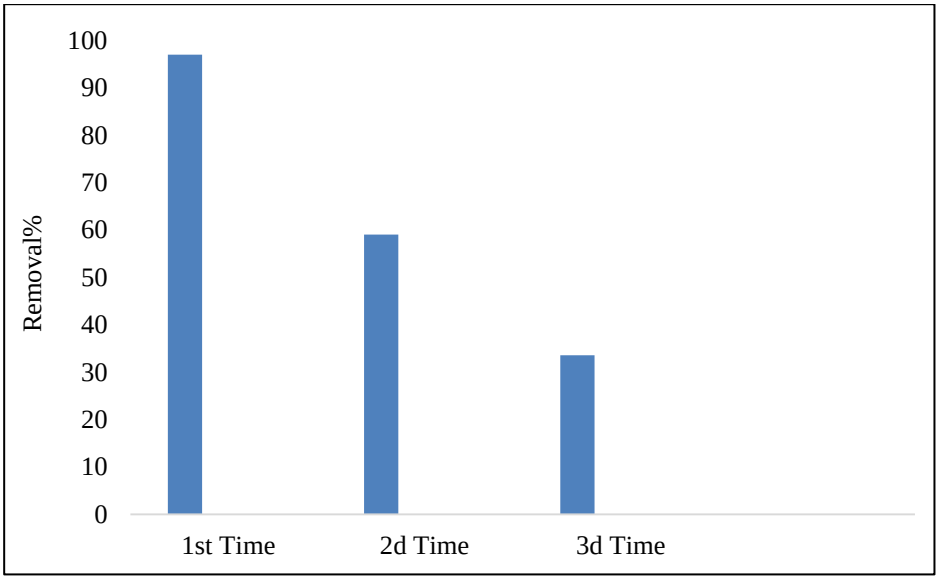

Figure 3.21: Results of magnetite-SLS MWCNTs regeneration over two cycles.

3.10. Carbon Nanotubes Cost Considerations and Large Scale Application

Carbon nanotubes proved to be promising adsorbent for heavy metals; they have higher adsorption capacity compared to conventional adsorbents. However, like any new material, carbon nanotubes are expensive which limits their application in large-scale industry [7]. Recently, results of different experimental studies revealed the possibility of producing high quality carbon nanotubes with lower cost [82]. Finding more economic techniques for mass production of carbon nanotubes will greatly help in its commercialization and make them economically feasible for large scale application.

\

Chapter 4. Conclusions and Recommendations

In this work, the various techniques used for the removal of heavy metals from wastewater with special focus on adsorption were firstly reviewed. This was followed by detailed discussion on adsorption equilibrium, kinetics, mechanisms and thermodynamics. Carbon nanotubes properties, chemical preparation, and applications were then presented. Furthermore, the previous studies in which carbon nanotubes were employed for heavy metals removal were also discussed and summarized. It was concluded that adsorption is a powerful method for heavy metals removal due to its technical and economic merits over other available methods. Various studies in the literature demonstrated that carbon nanotubes gave good results in the removal of selected heavy metals. However, the problem with carbon nanotubes is their tendency to agglomerate and form bundles in aqueous solutions which reduce their surface area and consequently affect their adsorption efficiency.

In this study, pristine MWCNTs were firstly tested for the removal of lead from aqueous solutions. Optimum values of adsorbent dosage, contact time, pH, and temperature using raw MWCNTs were found to be 15 g/L, 50 min, 6.5 and 25 ℃, respectively. In order to overcome the abovementioned shortcomings of MWCNTs, surface modification using sodium lauryl sulfate (SLS) was applied to the pristine MWCNTs so that sodium lauryl sulfate-multiwall carbon nanotubes (SLS-MWCNs) complex was obtained. SLS-MWCNTs were characterized using EDS, TGA and FTIR. Results showed that the surface was successfully modified. The SLS-MWCNTs were then tested on the removal of lead. Optimum values of adsorbent dosage, contact time, pH and temperature using SLS-MWCNTs were found to be 3 g/L, 30 min, 5.3 and 25 ℃, respectively. The best isotherm model in describing the raw-MWCNTs is the Langmuir model with maximum adsorption capacity of 3.84 mg/g. On the other hand, the best isotherm model in describing the SLS-MWCNTs is Freundlich model and the adsorption capacity calculated from it at 700 ppm is 141 mg/g. Furthermore, kinetics study revealed that both raw and SLS-MWCNTs follow pseudo second order kinetic model with rate constant of 0.11 g/mg.min and 0.06 g/mg.min, respectively. Thermodynamic study was also carried out and the results revealed that the adsorption of lead by raw-MWCNTs is endothermic while that of

SLS-MWCNTs is exothermic. However, the mode of adsorption on the surface of both adsorbents is physisorption.

In order to increase the density of the adsorbents, magnetite pellets of SLS-MWCNTs were prepared, characterized using FTIR and used in batch experiments. Results revealed that the efficiency of SLS-MWCNTs is not affected by the magnetation. Thus, the magnetite pellets were used in packed bed column. Column operation modelling results showed that modified dose response model is the best model in describing the column data. Regeneration for the saturated magnetite SLS-MWCNTs was done by treating it using 0.7 M HNO_3. The adsorption-desorption cycles were performed twice and the results showed that the removal percentage dropped from 97.1% to 59.1% for the first cycle and from 59.1% to 33.6% for the second cycle. Therefore, it is recommended to find more efficient method for regeneration such as KCl or higher concentration of nitric acid coupled with heating cycle.

References

[1] R. M. Brooks, M. Bahadory, F. Tovia and H. Rostami, "Removal of lead from contaminated water," *International Journal of Soil, Sediment and Water*, vol. 3 (2), Art No. 14, pp. 1-13, Jan, 2010.

[2] V. C. Renge, S. V. Khedkar and S. V. Pande, " Removal of heavy metals from wastewater using low cost adsorbents: a review," *Sci. Revs. Chem. Commun*, vol. 2, pp. 580-584, 2012.

[3] M. A. Barakat, "New trends in removing heavy metals from industrial wastewater," *Arabian Journal of Chemistry*, vol. 4, pp. 361-377, Jul 2010.

[4] N. G. Jern, *Industrial Wastewater Treatment*, Singapore: Imperial College Press, 2006.

[5] B. A. Oghenerobor, O. O. Gladys, D. O. Tomilola, "Heavy metal pollutants in wastewater effluents: Sources, effects and remediation," *Advances in Bioscience and Bioengineering*, vol. 2, pp. 37-43, 2014.

[6] F. L. Fu and Q. Wang, "Removal of heavy metal ions from wastewaters: A review," *Journal of Environmental Management*, vol. 92, pp. 407-418, Mar 2011.

[7] I. Ihsanullah, A. Abbas, A. M. Al-Amer, T. Laoui, M. J. Al-Marri, M. S. Nasser, M. Khraisheh, and M. A. Atieh, "Heavy metal removal from aqueous solution by advanced carbon nanotubes: Critical review of adsorption applications," *Separation and Purification Technology*, vol. 157, pp. 141–161, Sep 2015.

[8] H. M. Salem, E. M. Eweida and A. Farag, "Heavy metals in drinking water and their environmental impact on human health," *ICEHM2000*, pp. 542- 556, Sep 2000, Egypt.

[9] N. K. Srivastava and C. B. Majumder, "Novel biofiltration methods for the treatment of heavy metals from industrial wastewater," *J. Hazard. Mater*, vol. 151, pp. 1-8, 2008.

[10] L. G. Fernandez and H. Y. Olalla, "Toxicity and bioaccumulation of lead and cadmium in marine protozoan communities," *Ecotoxicology and Environmental Safety*, vol. 47, pp. 266-276, 2000.

[11] J. I. Gardea-Torresdey, J. R. Peralta-Videa, G. D. Rosa and J. G. Parsons, "Phytoremediation of heavy metals and study of the metal coordination by X-ray" *absorption spectroscopy*, vol. 249, pp. 1797-1810, 2005.

[12] A. Duda-Chodak and U. Blaszczyk, "The impact of nickel on human health," *Journal of Elementology*, vol. 13, pp. 685-696, Dec 2008.

[13] C. V. Mohod and J. Dhote, " Review of heavy metals in drinking water and their effect on human health," *International Journal of Innovative Research in Science, Engineering and Technology*, vol. 2, pp. 2992-2996, July 2013.

[14] A. T. Paulino, F. S. Minasse, M. R. Guilherme, A. V. Reis, E. C. Muniz and J. Nozaki, "Novel adsorbent based on silkworm chrysalides for removal of heavy metals from wastewaters," *J. Colloid Interface Sci*, vol. 301, pp. 479-487, 2006.

[15] J. O. Duruibe, M. O. Ogwuegbu and J. N. Egwurugwu, "Heavy metal pollution and human biotoxic effects," *International Journal of Physical Sciences*, vol. 2, pp. 112-118, 2007.

[16] F. F. Luqueño, F. L. Valdez, P. G. Melo, *et al.*, "Heavy metal pollution in drinking water - a global risk for human health: A review," *African Journal of Environmental Science and Technology*, vol. 7, pp. 567-584, July 2013.

[17] Guidelines for drinking-water quality - 4th ed. WHO Library Cataloguing-in-Publication Data, World Health Organization, 2011.

[18] R. Naseem and S. S. Tahir, "Removal of Pb(II) from aqueous solution by using bentonite as an adsorbent," *Water Res*. vol. 35, pp. 3982-3986, 2001.

[19] United States Environmental Protection Agency, Table of regulated drinking water contaminants. Available: http://www.epa.gov/your-drinking-water/table-regulated-drinking-water-contaminants # Inorganic [Accessed: 17 June 2016].

[20] L. Khezami and R. Capart, "Removal of chromium (VI) from aqueous solution by activated carbons: kinetic and equilibrium studies," *J. Hazard. Mater*, vol. 123, pp. 223-231, 2005.

[21] I. Ihsanullah, F. A. A. Khaldi, B. A. Sharkh, A. M. Abulkibash, M. I. Qureshi, T. Laoui and M. A. Atieh, "Effect of acid modification on adsorption of hexavalent chromium (Cr(VI)) from aqueous solution by activated carbon and carbon nanotubes," *Desalin. Water Treat*, vol. 57, pp. 7232–7244, 2015.

[22] C. Namasivayam and K. Kadirvelu, "Uptake of mercury (II) from wastewater by activated carbon from unwanted agricultural solid by-product: coirpith," *Carbon*. vol 37, pp. 79-84, 1999.

[23] Zinc in drinking-water, Background document for development of WHO guidelines for drinking-water quality, Originally published in Guidelines for drinking-water quality, 2nd ed. vol. 2. Health criteria and other supporting information. World Health Organization, Geneva, 1996.

[24] E. A. Deliyanni, E. N. Peleka and K. A. Matis, "Removal of zinc ion from water by sorption onto iron-based nanoadsorbent," *J. Hazard.Mater*. vol. 141, pp. 176–184, 2007.

[25] S. T. Yang, J. X. Li, D. D. Shao, J. Hu and X. K. Wang, "Adsorption of Ni(II) on oxidized multi-walled carbon nanotubes: effect of contact time, pH, foreign ions and PAA," *J. Hazard. Mater*, vol. 166, pp. 109–116, 2009.

[26] S. A. Mirbagherp and S. N. Hosseini, "Pilot plant investigation on petrochemical wastewater treatment for the removal of copper and chromium with the objective of reuse," *Desalination*, vol. 171, pp. 85–93, 2004.

[27] B. Alyüz, and S. Veli, "Kinetics and equilibrium studies for the removal of nickel and zinc from aqueous solutions by ion exchange resins," *J. Hazard. Mater*. vol. 167, pp. 482-488, 2009.

[28] Q. Chang and G. Wang, "Study on the macromolecular coagulant PEX which traps heavy metals," *Chem. Eng. Sci*, vol. 62, pp. 4636–4643, 2007.

[29] S. Vigneswaran, H. H. Ngo, D. S Chaudhary and Y. T. Hung, "Physico-chemical treatment processes for water reuse." in: Wang, L. K., Hung, Y.T., Shammas, N.K. (Eds.), *Physicochemical Treatment Processes*, 3d ed. New Jersey, Humana Press, 2004, ch. 16, pp. 635–676.

[30] N. Hilal, H. Al-Zoubi, N. A. Darwish, A. W. Mohammad and M. Abu Arabi, "A comprehensive review of nanofiltration membranes: Treatment, pretreatment, modelling, and atomic force microscopy," *Desalination*, vol. 170, pp. 281-308, 2004.

[31] R. W. Peters and Y. Ku, "Evaluation of recent treatment techniques for removal of heavy metals from industrial wastewaters," *AlChE Symposium Series*, vol. 81, pp. 165-203, Sep 1985.

[32] J. F. Richardson, J. H. Harker and J. R. Backhurst, "Adsorption." in *Particle Technology and Separation Processes*. 5th ed. Butterworth-Heinemann, 2002.

[33] C. J. Geankoplis, "Liquid-liquid and fluid-solid separation processes." In *Transport Processes and Unit Operation*s. 3d ed. New Jersey, Prentice-Hall International, Inc, 1993.

[34] L. A. Tan and B. H. Hameed, "Adsorption isotherms, kinetics, thermodynamics and desorption studies of basic dye on activated carbon derived from oil palm empty fruit bunch, *Journal of Applied Science*, vol. 10 (21), pp. 2565-2571, 2010.

[35] A. Dabrowski, "Adsorption - from theory to practice," *Advances in Colloid and Interface Science*, vol. 93, pp. 135-224, Sep 2001.

[36] Y. S. Ho, J. F. Porter and G. Mckay, "Equilibrium isotherm studies for the sorption of divalent metal ions onto peat: Copper, nickel and lead single component systems," *Water, Air, and Soil Pollution*, vol. 141, pp. 1–33, 2002.

[37] Xunjun Chen, "Modeling of experimental adsorption isotherm data," *Information*, vol. 6, ISSN 2078-2489, pp 14-22, Jan 2015.

[38] A. O. Dada, A. P. Olalekan, A. M. Olatunya and O. DADA, "Langmuir, Freundlich, Temkin and Dubinin–Radushkevich isotherms studies of equilibrium sorption of Zn^{+2} unto phosphoric acid modified rice husk," *IOSR Journal of Applied Chemistry* (IOSR-JAC), vol. 3, pp. 38-45, Dec 2012.

[39] Nahid Ghasemi, Sara Mirali, Maryam Ghasemi, Somaye Mashhadi and Mohammad HadiTarraf , "Adsorption isotherms and kinetics Studies for the removal of Pb(II) from Aqueous Solutions using Low-cost adsorbent," *International Conference on Environment Science and Engineering* IPCBEE vol. 32, pp. 79-83, 2012, Singapoore.

[40] S. M. Yakout and E. Elsherif, "Batch kinetics, isotherm and thermodynamic studies of adsorption of strontium from aqueous solutions onto low cost rice-straw based carbons," *Carbon – Sci. Tech*. vol. 3, pp. 144-153, 2010.

[41] Y. S. Ho, "Review of second-order models for adsorption systems," *Journal of Hazardous Materials*, vol. 136, pp. 681–689, 2006.

[42] B. H. Hameed, D. K. Mahmoud and A. L. Ahmad, "Equilibrium modeling and kinetic studies on the adsorption of basic dye by a low-cost adsorbent: Coconut (Cocosnucifera) bunch waste," *Journal of Hazardous Materials*, vol. 158, pp. 65–72, 2008.

[43] A. Mittal, V. Gajbe and J. Mittal, "Removal and recovery of hazardous triphenylmethane dye, methyl violet through adsorption over granulated wastematerials," *J. Hazard. Mater*, vol. 150, pp. 364-375.

[44] T. Tarawou and E. Young, "Intraparticle and liquid film diffusion studies on the adsorption of Cu^{2+} and Pb^{2+} ions from aqueous solution using powdered cocoa pod (Theobroma cacao),"*International Research Journal of Engineering and Technology*, vol. 2, pp. 236-243, 2015.

[45] R. Subha and C. Namasivayam, "Modeling of adsorption isotherms and kinetics of 2,4,6 trichlorophenol onto microporous $ZnCl_2$ activated coir pith carbon," *J. Environ. Eng. Manage*, vol. 18, pp. 275-280, 2008.

[46] M. Dakiky, M. Khamis, A. Manassra, and M. Mer'eb, "Selective adsorption of chromium(VI) in industrial wastewater using low-cost abundantly available

adsorbents," *Advances in environmental research : an international journal of research in environmental science, engineering and technology,* vol. 6, pp. 533-540, 2002.

[47] M. A. Alanber, "Thermodynamics approach in the adsorption of heavy metals," in Juan Carlos Moreno PirajÃ¡n. *Thermodynamics - Interaction Studies - Solids, Liquids and Gases*, InTech, 2011, ch. 27, pp. 737-764.

[48] T. A. Kurniawan, G.Y.S. Chan, W. H. Lo, S. Babel, "Comparisons of low-cost adsorbents for treating wastewaters laden with heavy metals," *Sci. Total Environ*. vol. 366, pp. 409–426, 2005.

[49] Y. H. Li, Y. M. Zhao, W. B. Hu, I. Ahmad, Y. Q. Zhu, X. J. Peng and Z. K. Luan, "Carbon nanotubes – the promising adsorbent in wastewater treatment," *Journal of Physics: Conference Series*, vol. 61, pp. 698–702, 2007.

[50] A. Eatemadi, H. Daraee, H. Karimkhanloo, M. Kouhi, N. Zarghami, A. Akbarzadeh, M. Abasi, Y. Hanifehpour and S. Joo "Carbon nanotubes: properties, synthesis, purification, and medical applications," *Nanoscale Research Letters,* vol. 9, pp. 393/ 1-13, Aug 2014.

[51] N. Valentin "Carbon nanotubes: properties and application**,**" *Materials Science and Engineering*, vol. 43, pp. 61-102, 2004.

[52] M. Terrones, "Science and technology of the twenty-first century: synthesis, properties and applications of carbon nanotubes," *Annual Review of Materials Research,* vol. 33, pp. 419-501, 2003.

[53] M. F. L. De Volder, S. H. Tawfick, R. H. Baughman, and A. J. Hart, "Carbon nanotubes: present and future commercial applications," *Science,* vol. 339, pp. 535-539, Feb 2013.

[54] S. Agnihotri, M. Rostam-Abadi, M. J. Rood, and R. Chang, "Energy and environmental applications of carbon nanotubes," *Abstracts of Papers of the American Chemical Society*, vol. 224, pp. U560-U560, Aug 2002.

[55] K. S. Ibrahim, "Carbon nanotubes–properties and applications: a review," *Carbon letters*, vol. 14, no. 3, pp. 131–144, 2013.

[56] Min-Feng Yu, Oleg Lourie, Mark J. Dyer, Katerina Moloni, Thomas F. Kelly and Rodney S. Ruoff1, " Strength and breaking mechanism of multiwalled carbon nanotubes under tensile load," *Science*, vol. 287, pp. 637-640, 2000.

[57] B. K. Kaushik and M. K. Majumder, "Carbon nanotube: properties and applications," in *Carbon Nanotube Based VLSI Interconnects: Analysis and Design*, Springer Briefs in Applied Sciences and Technology, 2015, ch. 2, pp. 17-37.

[58] P. Kim, L. Shi, A. Majumdar, and P. L. McEuen, "Thermal transport measurements of individual multiwalled nanotubes," *Physical Review Letters*, vol. 87, issue. 21, pp. 215502/ 1-4, 2001.

[59] N. M. Mubarak, J. N. Sahu, E. C. Abdullah and N. S. Jayakumar, "Removal of heavy metals from wastewater using carbon nanotubes," *Separation & Purification Reviews*, vol. 43, pp. 311–338, 2014

[60] V. Mittal, "Carbon nanotubes surface modifications: an overview," in *Surface Modification of Nanotube Fillers*, 1st ed. John Wiley& Sons, 2011, ch. 1, pp. 1–23.

[61] Y. Wang, L. Shi, L. Gao, Q. Wei, L. Cui, L. Hu, L. Yan and B. Du, "The removal of lead ions from aqueous solution by using magnetic hydroxypropyl chitosan/oxidized multiwalled carbon nanotubes composites," *Journal of Colloid and Interface Science*, vol. 451, pp. 7–14, Aug 2015.

[62] Yan-Hui Li , Jun Ding , Zhaokun Luan , Zechao Di , Yuefeng Zhu , Cailu Xu , Dehai Wu and Bingqing Wei, "Competitive adsorption of Pb , Cu and Cd ions from aqueous solutions by multiwalled carbon nanotubes," *Journal of Carbon*, vol. 41, pp. 2787–2792, Aug 2003.

[63] G. D. Vukovic, A. D. Marinkovic, S. D. Skapin, M. D. Ristic, R. Aleksic, A. A. Peric-Grujic and P. S. Uskoković, "Removal of lead from water by amino modified multi-walled carbon nanotubes," *Chemical Engineering Journal*, vol. 173, pp. 855-865, Oct 2011.

[64] M. A. Salam, G. Al-Zhrani, and S. A. Kosa, "Simultaneous removal of copper(II), lead(II), zinc(II) and cadmium(II) from aqueous solutions by multi-walled carbon nanotubes," *Comptes Rendus Chimie*, vol. 15, pp. 398-408, May 2012.

[65] M. A. Salam, "Coating carbon nanotubes with crystalline manganese dioxide nanoparticles and their application for lead ions removal from model and real water, "*Colloids and Surfaces a-Physicochemical and Engineering Aspects*, vol. 419, pp. 69-79, Feb 2013.

[66] J. X. Li, S. Y. Chen, G. D. Sheng, J. Hu, X. L. Tan and X. K. Wang, "Effect of surfactants on Pb(II) adsorption from aqueous solutions using oxidized multiwallcarbon nanotubes," *Chemical Engineering Journal*, vol. 166, pp. 551-558, Jan 2011.

[67] H. J. Wang, A. L. Zhou, F. Peng, H. Yu, and J. Yang, "Mechanism study on adsorption of acidified multiwalled carbon nanotubes to Pb(II)," *Journal of Colloid and Interface Science*, vol. 316, pp. 277-283, Dec 2007.

[68] H. J. Wang, A. L. Zhou, F. Peng, H. Yu, and L. F. Chen, "Adsorption characteristic of acidified carbon nanotubes for heavy metal Pb(II) in aqueous solution, "*Materials Science and Engineering a-Structural Materials Properties Microstructure and Processing*, vol. 466, pp. 201-206, Sep 2007.

[69] X. W. Zhao, Q. Jia, N. Z. Song, W. H. Zhou, and Y. S. Li, "Adsorption of Pb(II) from an aqueous solution by titanium dioxide/carbon nanotube nanocomposites: kinetics, thermodynamics, and isotherms," *Journal of Chemical and Engineering Data*, vol. 55, pp. 4428-4433, Oct 2010.

[70] M. S. Tehrani, P. A. Azar, P. E. Namin and S. M. Dehaghi, "Removal of lead ions from wastewater using functionalized multiwalled carbon nanotubes with tris(2-aminoethyl) amine" *Journal of Environmental Protection*, vol. 4, pp. 529-536, Jun 2013.

[71] M. Jahangiri, F. Kiani, H. Tahermansouri and A. Rajabalinezhad, "The removal of lead ions from aqueous solutions by modified multi-walled carbon nanotubes with 1-isatin-3-thiosemicarbazone" *Journal of Molecular Liquids*, vol. 212, pp. 219–226, Sep 2015.

[72] C. Zhang, J. H. Sui, J. Li, Y. L. Tang, and W. Cai, "Efficient removal of heavy metal ions by thiol-functionalized superparamagnetic carbon nanotubes," *Chemical Engineering Journal*, vol. 210, pp. 45-52, Nov 2012.

[73] A. Stafiej and K. Pyrzynska, "Adsorption of heavy metal ions with carbon nanotubes," *Separation and Purification Technology*, vol. 58, pp. 49–52, 2007.

[74] O. Kerkez-Kuyumcu, S. S. Bayazit, and M. A. Salam, "Antibiotic amoxicillin removal from aqueous solution using magnetically modified graphene nanoplatelets," *Journal of Industrial and Engineering Chemistry*, vol. 36, pp. 198-205, Apr 2016.

[75] "Infrared Spectroscopy Absorption Table," *Chemistry Libre Texts*, 21-Jul-2016. [Online].Available:https://chem.libretexts.org/Reference/Reference_Tables/Spectroscopic_Parameters/Infrared_Spectroscopy_Absorption_Table. [Accessed: 02-Apr-2017].

[76] O. Abdelwahab and N. K. Amin, "Adsorption of phenol from aqueous solutions by Luffa cylindrica fibers: kinetics, isotherm and thermodynamic studies," *The Egyptian Journal of Aquatic Research*, vol. 39, pp. 215-223, 2013.

[77] L. Largitte and R. Pasquier, "A review of the kinetics adsorption models and their application to the adsorption of lead by an activated carbon," *Chemical Engineering Research and Design*, vol. 109, pp. 495–504, 2016.

[78] M. A. P. Guzman, J. S. Salazar, R. O. Amaya, Y. Matsumoto, and M. O. Lopez, "Synthesis and characterization of magnetite-graphene oxide nanocomposite," *13th International Conference on Electrical Engineering, Computing Science and Automatic Control (CCE)*, 2016, Mexico.

[79] Z. Xu, J.-G. Cai, and B.-C. Pan, "Mathematically modeling fixed-bed adsorption in aqueous systems," *Journal of Zhejiang University SCIENCE A*, vol. 14, no. 3, pp. 155–176, 2013.

[80] A. P. Lim and A. Z. Aris, "Continuous fixed-bed column study and adsorption modeling: Removal of cadmium (II) and lead (II) ions in aqueous solution by dead calcareous skeletons," *Biochemical Engineering Journal*, vol. 87, pp. 50–61, 2014.

[81] P. R. Rout, R. R. Dash, and P. Bhunia, "Modelling and packed bed column studies on adsorptive removal of phosphate from aqueous solutions by a mixture of ground burnt patties and red soil," *Advances in environmental research*, vol. 3, no. 3, pp. 231–251, 2014.

[82] Y. T. Ong, A. L. Ahmad, S. H. S. Zein, and S. H. Tan, "A review on carbon nanotubes in an environmental protection and green engineering perspective," *Brazilian Journal of Chemical Engineering*, vol. 27, no. 2, pp. 227–242, 2010.

Appendix A

A.1. Isotherm Models Fitting

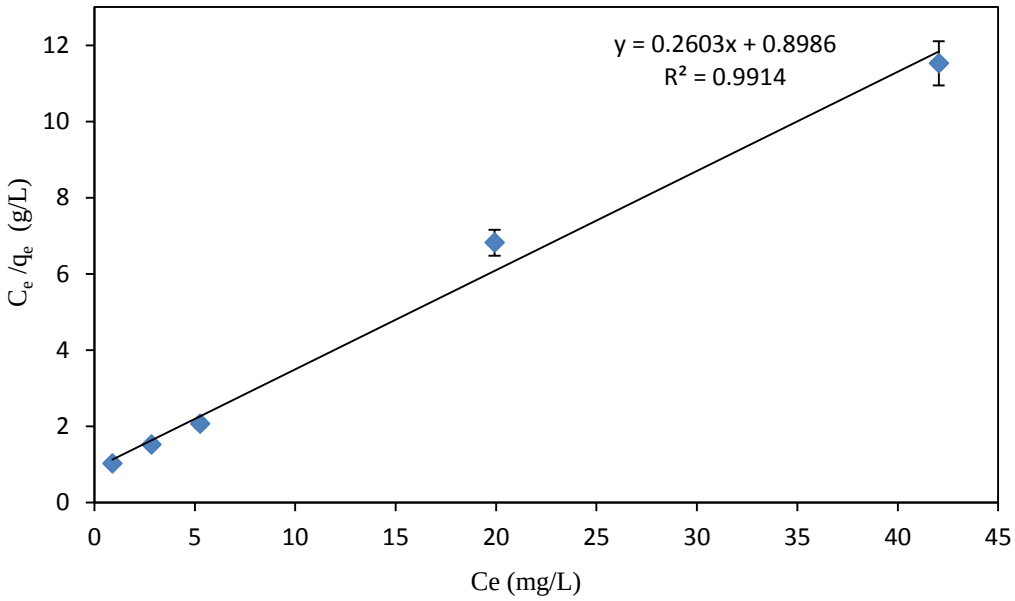

Figure A.1: Langmuir isotherm model for adsorption of lead using raw-MWCNTs.

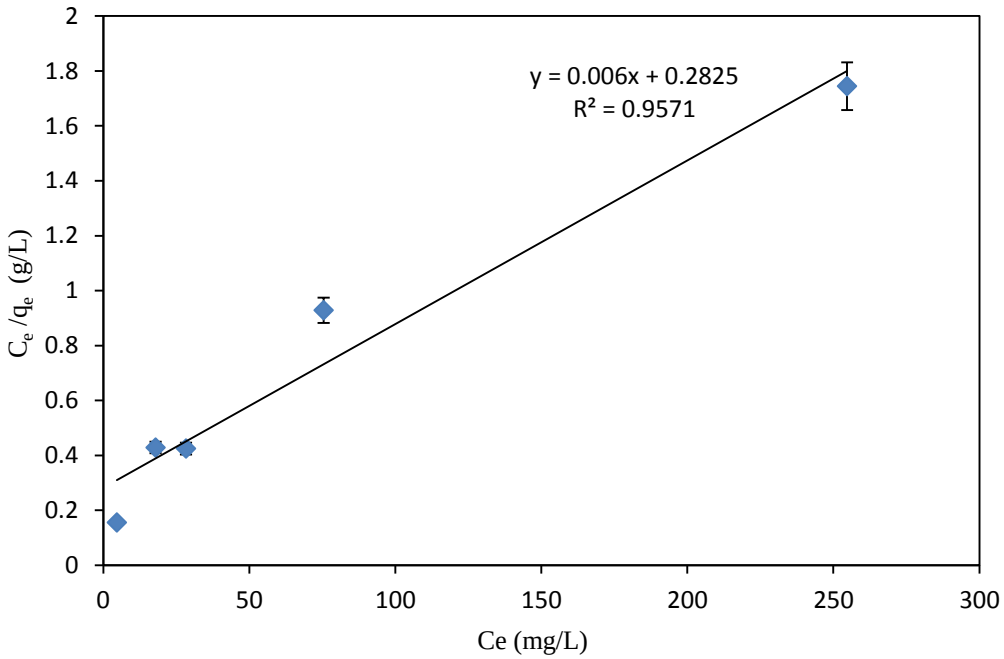

Figure A.2: Langmuir isotherm model for adsorption of lead using SLS-MWCNTs.

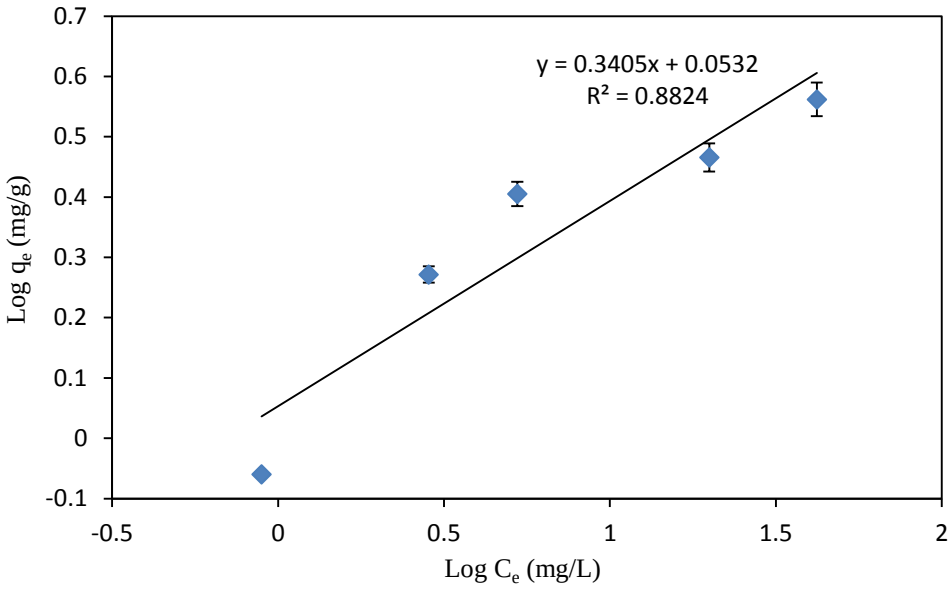

Figure A.3: Freundlich isotherm model for adsorption of lead using raw-MWCNTs.

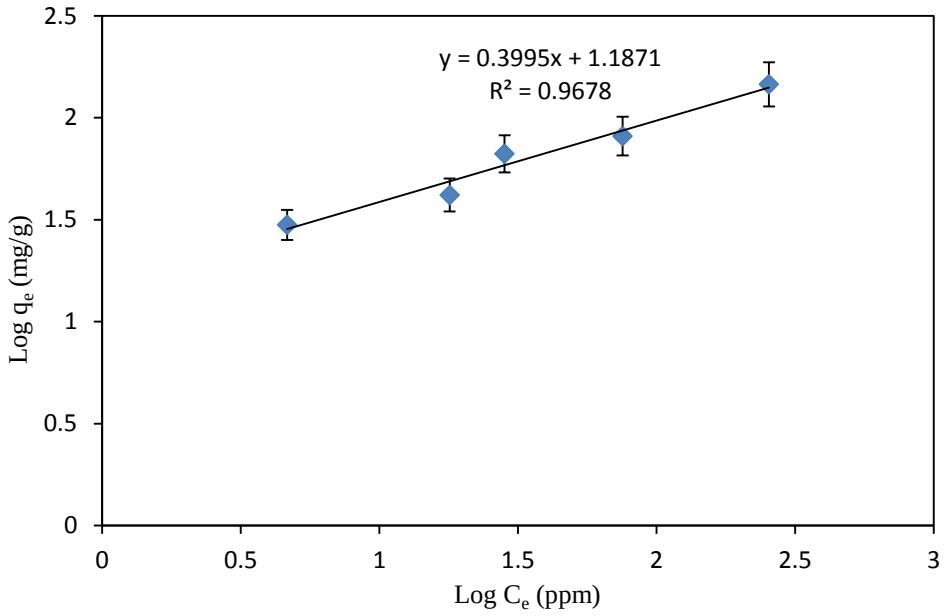

Figure A.4: Freundlich isotherm model for adsorption of lead using SLS-MWCNTs.

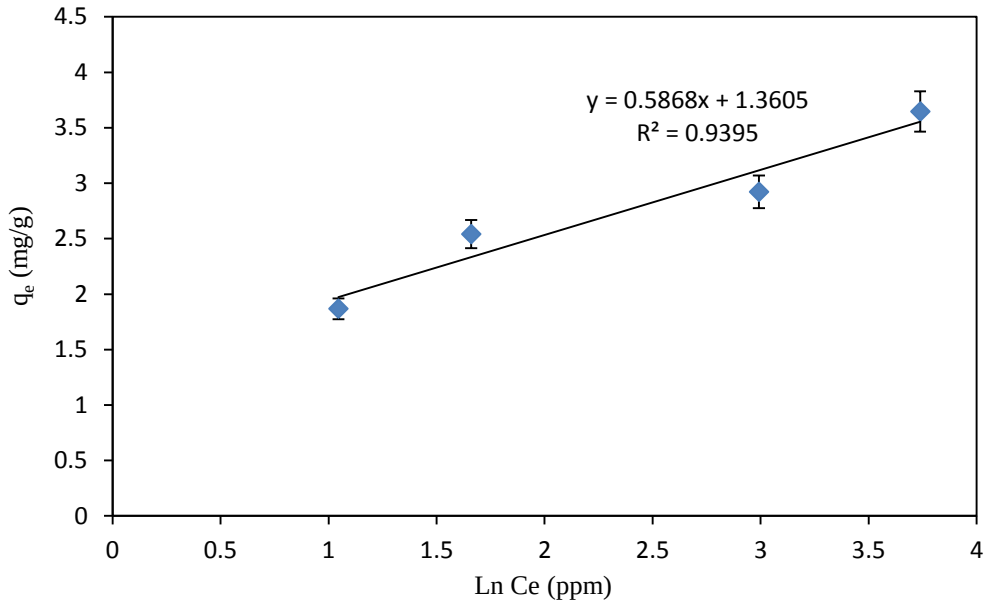

Figure A.5: Temkin isotherm model for adsorption of lead using raw-MWCNTs.

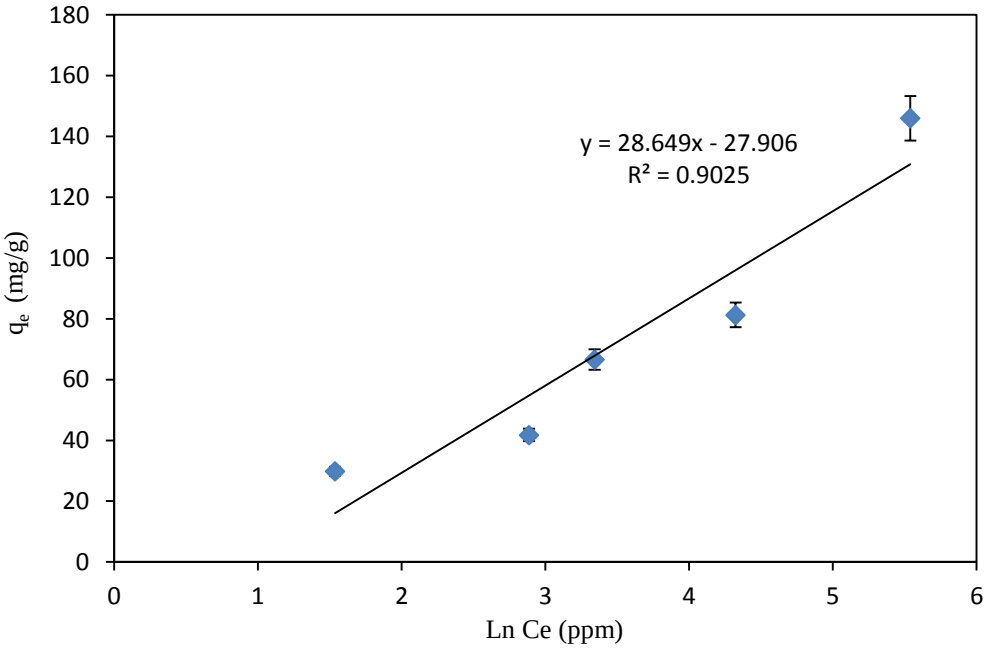

Figure A.6: Temkin isotherm model for adsorption of lead using SLS-MWCNTs.

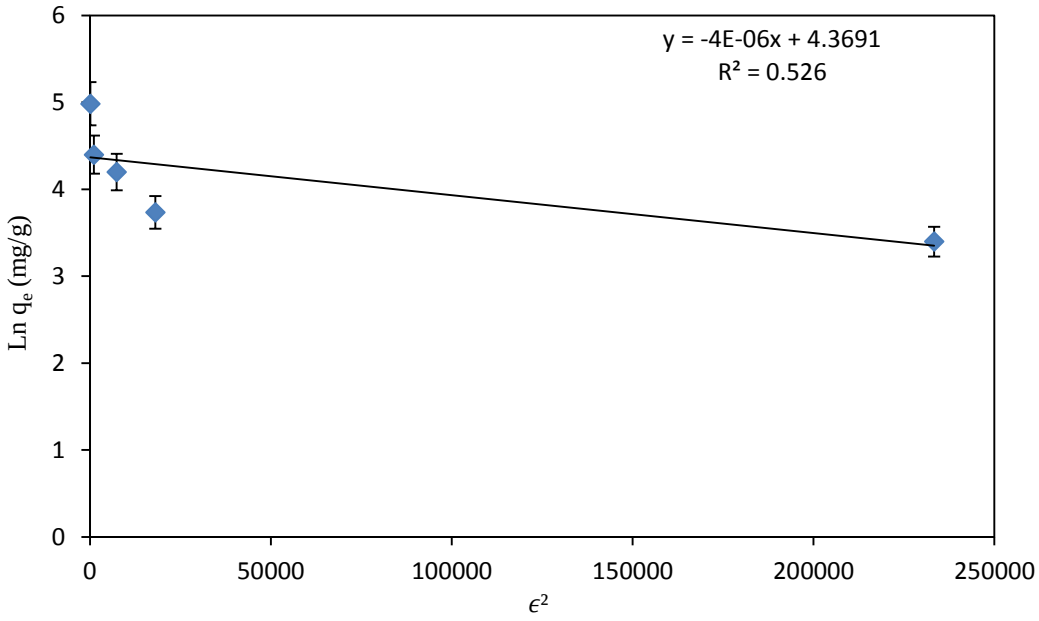

Figure A.7: D-R isotherm model for adsorption of lead using raw-MWCNTs.

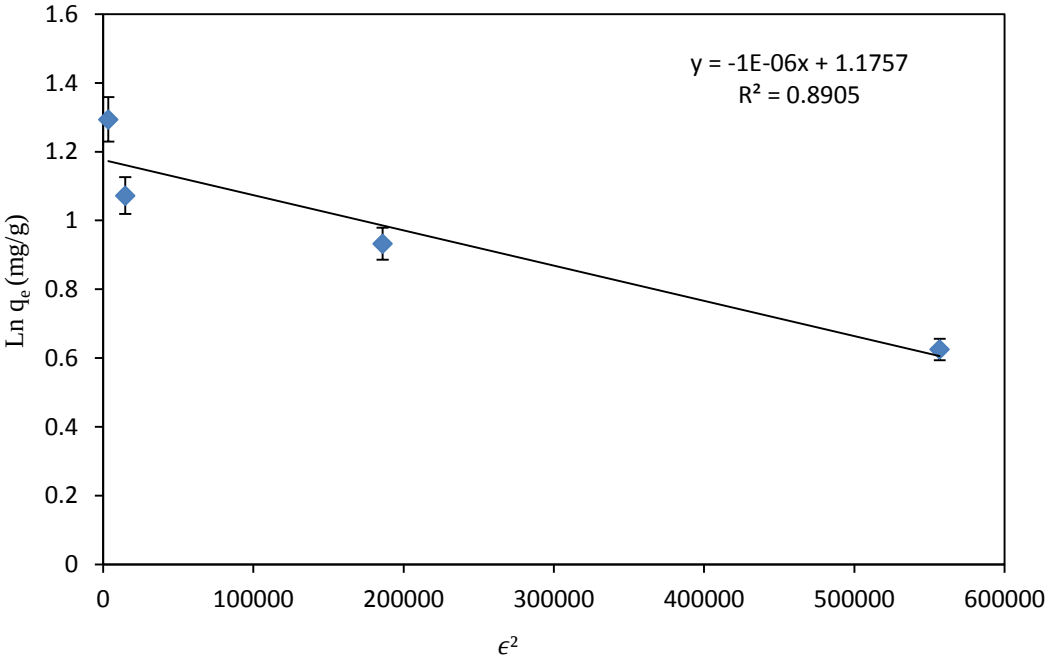

Figure A.8: D-R isotherm model for adsorption of lead using SLS-MWCNTs.

A.2. Kinetic Models Fitting

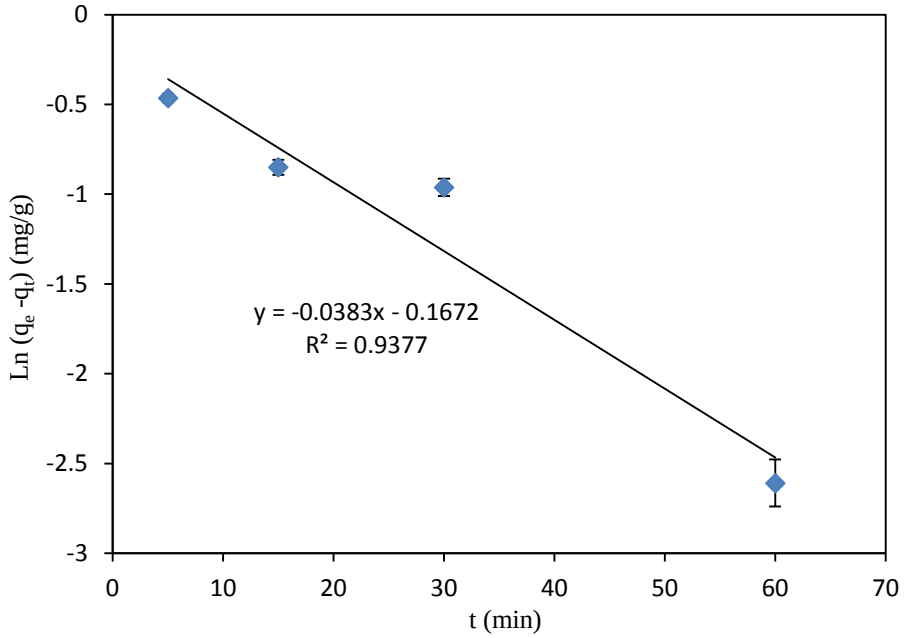

Figure A.9: Pseudo- first order model for lead adsorption using raw-MWCNTs.

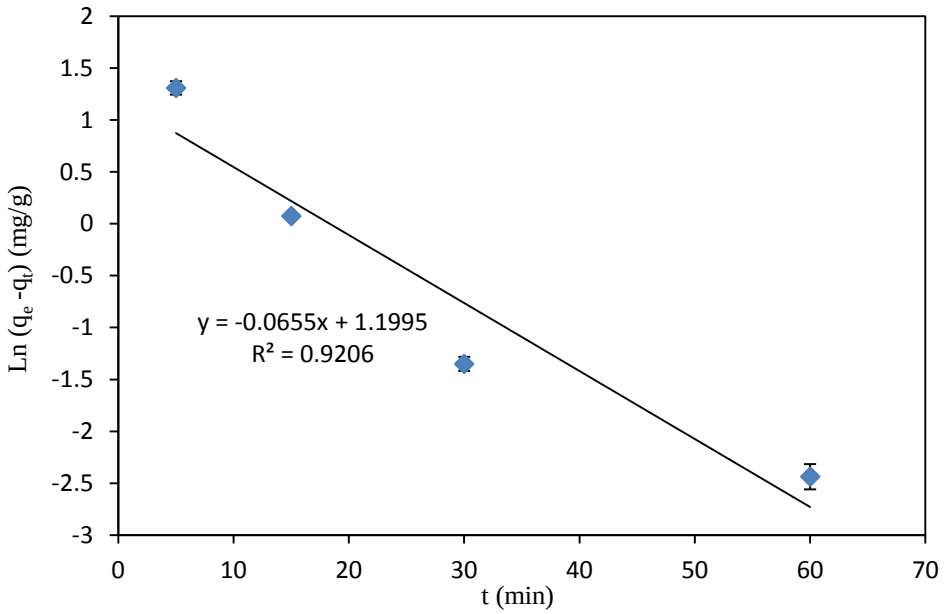

Figure A.10: Pseudo- first order model for lead adsorption using SLS-MWCNTs.

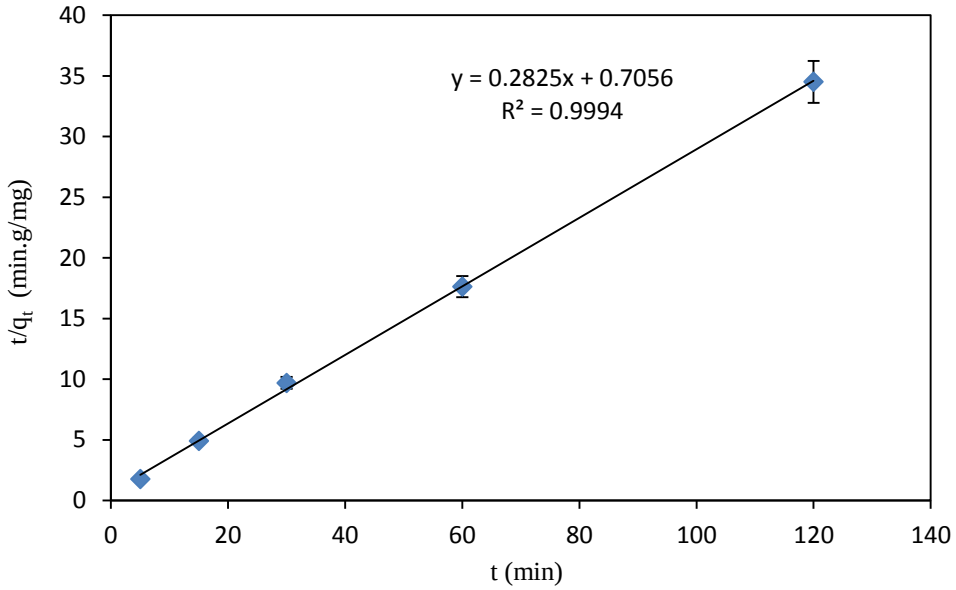

Figure A.11: Pseudo- second order model for lead adsorption using raw-MWCNTs.

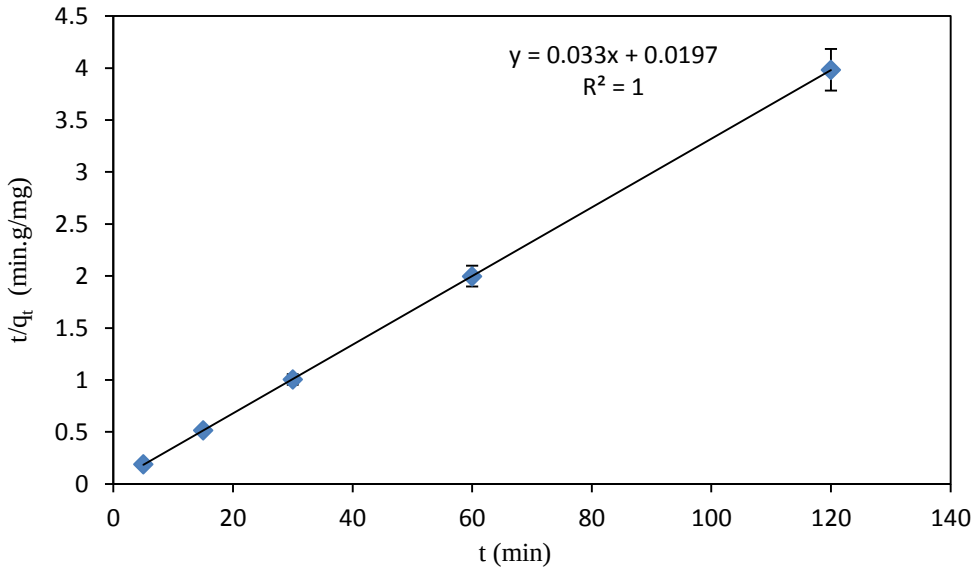

Figure A.12: Pseudo- second order model for lead adsorption using SLS-MWCNTs.

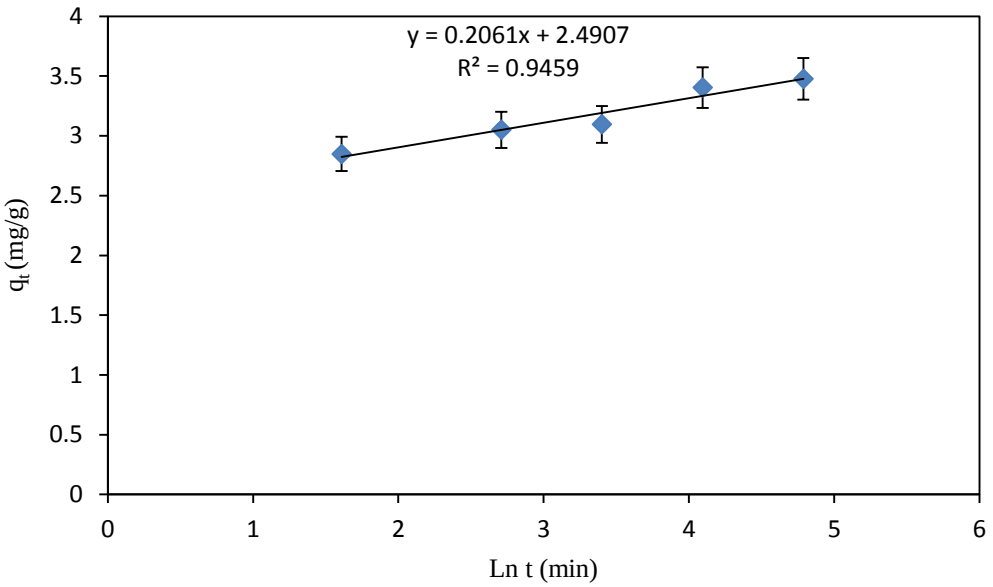

Figure A.13: Elovich model for lead adsorption using raw-MWCNTs.

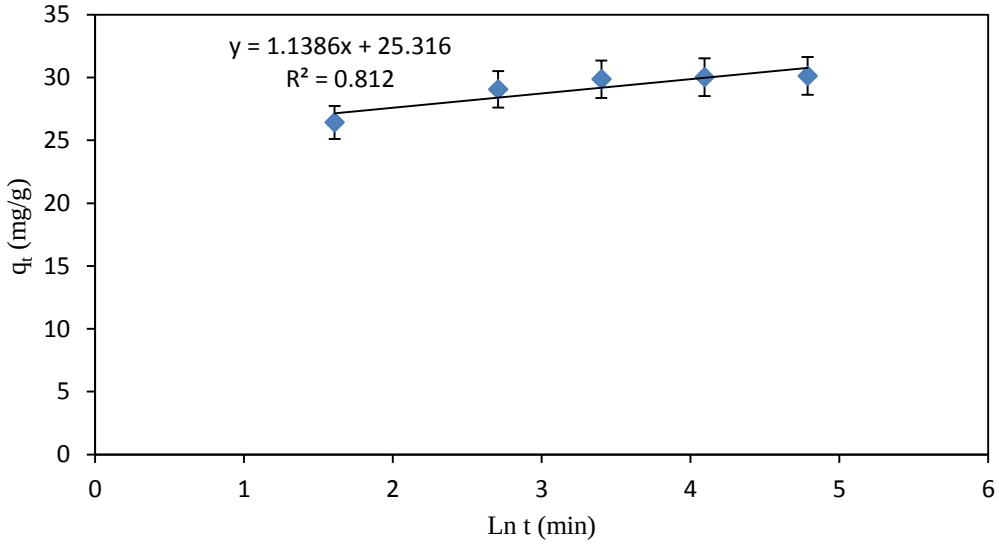

Figure A.14: Elovich model for lead adsorption using SLS-MWCNTs.

A.3. Van't Hoff Plots

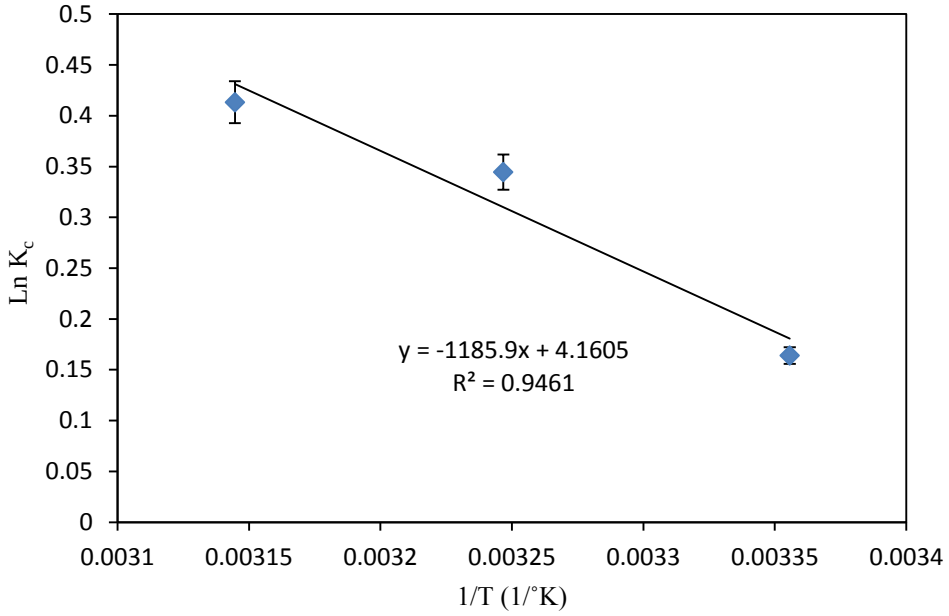

Figure A.15: Van't Hoff plot of ln K_c vs I/T for the adsorption of lead on raw MWCNTs.

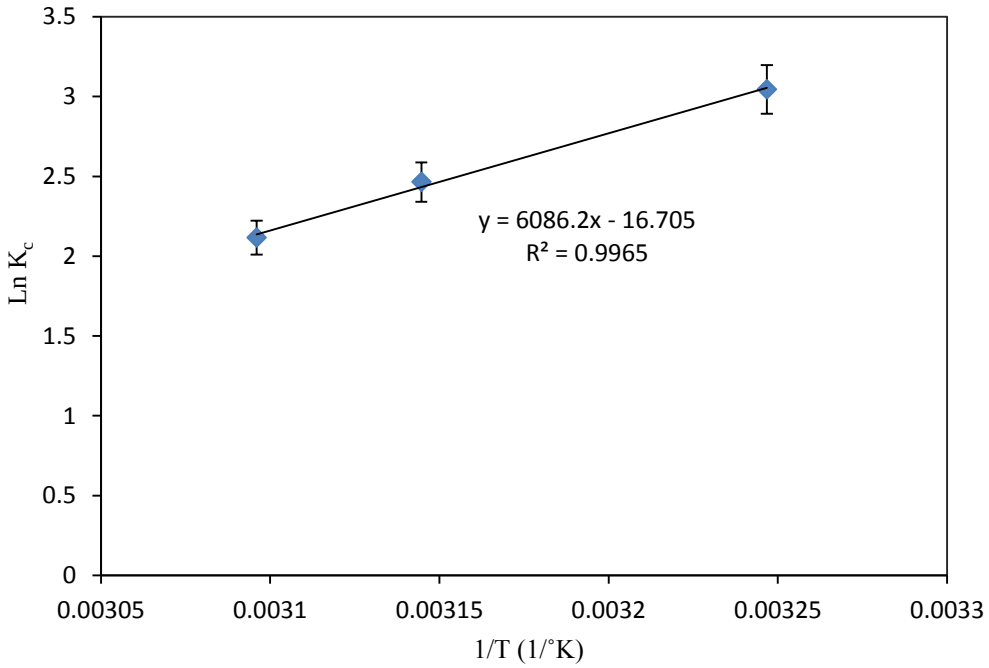

Figure A.16: Van't Hoff plot of ln K_c vs I/T for the adsorption of lead on SLS MWCNTs.

A.4. Fixed Bed Column Models Fitting

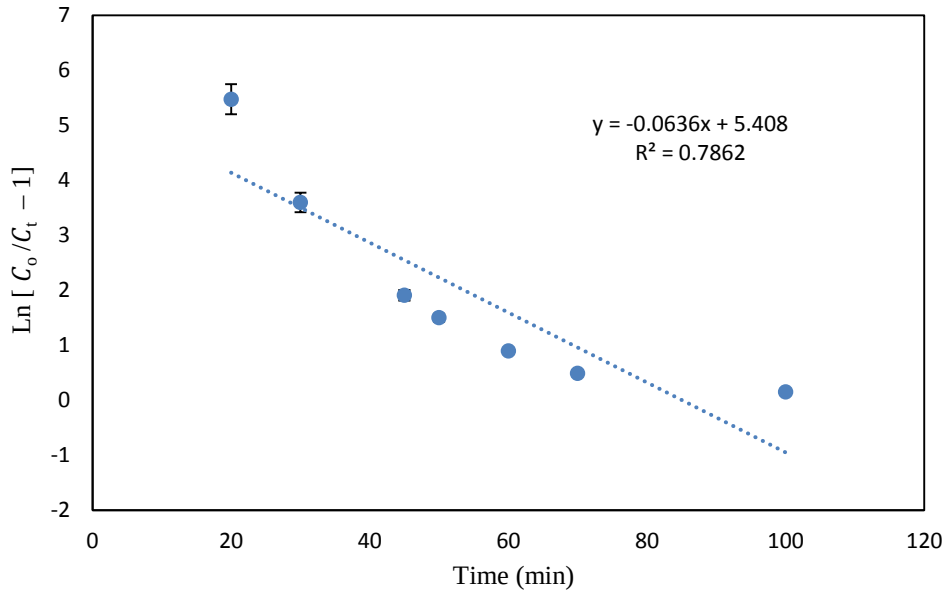

Figure A.17: Fitting of column data on Thomas model.

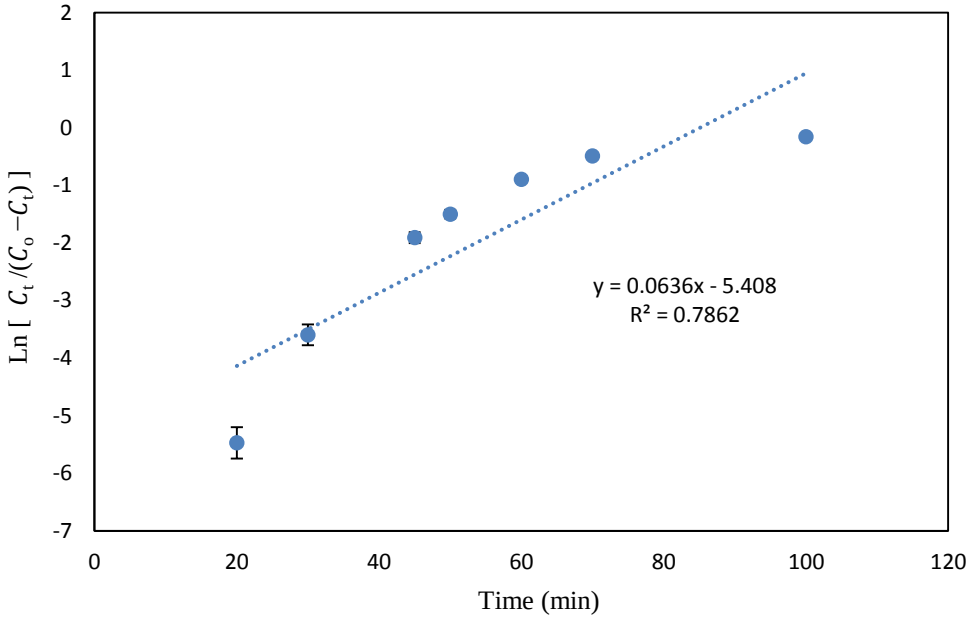

Figure A.18: Fitting of column data on Yoon-Nelson model.

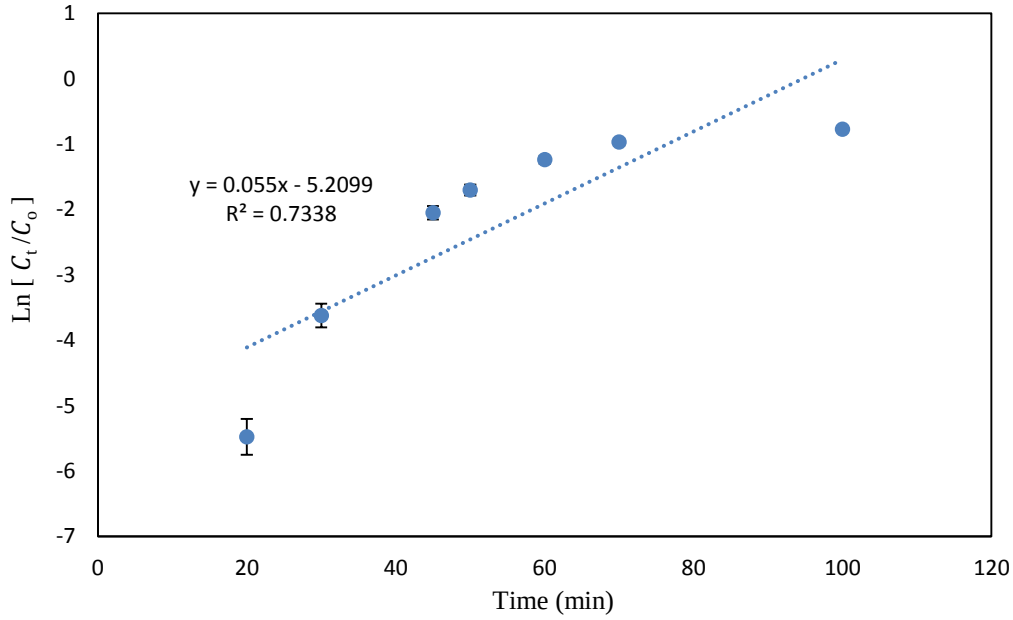

Figure A.19: Fitting of column data on Adam-Bohart model.

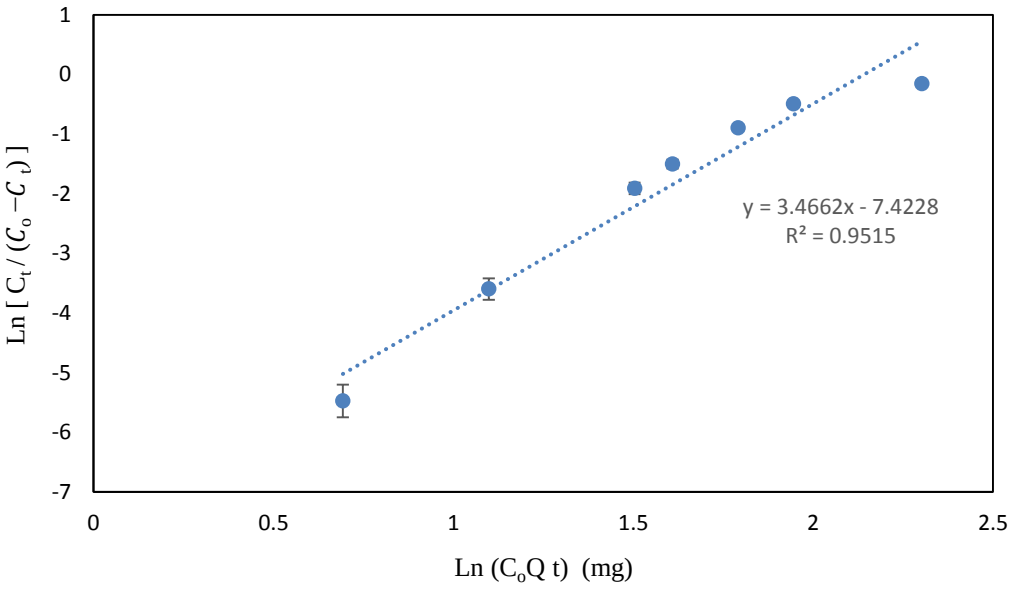

Figure A.20: Fitting of column data on MDR model.

Vita

Malaz Suliman was born in 1991, in Khartoum, Sudan. She was educated in local schools and graduated from high school in 2007. She studied at the University of Khartoum and graduated with first class in 2012. Her degree was a Bachelor of Science in Chemical Engineering. In Fall 2015, she joined the Chemical Engineering master's program at the American University of Sharjah where she was awarded a full graduate teaching assistantship.